Inorganic Chemistry

ARTICLE

pubs.acs.org/IC

New Heteroleptic Bis-Phenanthroline Copper(I) Complexes with Dipyridophenazine or Imidazole Fused Phenanthroline Ligands: Spectral, Electrochemical, and Quantum Chemical Studies

Yann Pellegrin,[†] Martina Sandroni,[†] Errol Blart,[†] Aurélien Planchat,[†] Michel Evain,[*,§] Narayan C. Bera,[‡] Megumi Kayanuma,[‡] Michel Sliwa,[*,∥] Mateusz Rebarz,[∥] Olivier Poizat,[∥] Chantal Daniel,[*,‡] and Fabrice Odobel[*,†]

[†]CEISAM, Université de Nantes, CNRS, 2 rue de la Houssinière, 44322 Nantes Cedex 3, France

[‡]Laboratoire de Chimie Quantique, Institut de Chimie, UMR 7177 CNRS-Université de Strasbourg, 4 rue Blaise Pascal, CS 90032, F-67081 Strasbourg Cedex, France

[§]IMN, Université de Nantes, CNRS, 2 rue de la Houssinière, 44322 Nantes Cedex 3, France

[∥]Laboratoire de Spectrochimie Infrarouge et Raman, UMR 8516 CNRS-Université Lille 1 Sciences et Technologies, 59655 Villeneuve d'Ascq Cedex, France

Supporting Information

ABSTRACT: Two new sterically challenged diimine ligands $\mathbf{L_1}$ (2,9-dimesityl-2-(4′-bromophenyl)imidazo[4,5-*f*][1,10]phenanthroline) and $\mathbf{L_2}$ (3,6-di-*n*-butyl-11-bromodipyrido[3,2-*a*:2′,3′-*c*]phenazine) have been synthesized with the aim to build original heteroleptic copper(I) complexes, following the HETPHEN concept developed by Schmittel and co-workers. The structure of $\mathbf{L_1}$ is based on a phen-imidazole molecular core, derivatized by two highly bulky mesityl groups in positions 2 and 9 of the phenanthroline cavity, preventing the formation of a homoleptic species, while $\mathbf{L_2}$ is a dppz derivative, bearing *n*-butyl chains in α positions of the chelating nitrogen atoms. The unambiguous formation of six novel heteroleptic copper(I) complexes based on $\mathbf{L_1}$, $\mathbf{L_2}$, and complementary matching ligands (2,9-R_2-1,10-phenanthroline, with R = H, methyl, *n*-butyl or mesityl) has been evidenced, and the resulting compounds were fully characterized. The electronic absorption spectra of all complexes fits well with DFT calculations allowing the assignment of the main transitions. The characteristics of the emissive excited state were investigated in different solvents using time-resolved single photon counting and transient absorption spectroscopy. The complexes with ligand $\mathbf{L_2}$, bearing a characteristic dppz moiety, exhibit a very low energy excited-state which mainly leads to fast nonradiative relaxation, whereas the emission lifetime is higher for those containing the bulky ligand $\mathbf{L_1}$. For example, a luminescence quantum yield of about 3×10^{-4} is obtained with a decay time of about 50 ns for **C2** ($[Cu^{I}(nBu\text{-}phen)(\mathbf{L_1})]^{+}$) with a weak influence of strong coordinating solvent on the luminescence properties. Overall, the spectral features are those expected for a highly constrained coordination cage. Yet, the complexes are stable in solution, partly due to the beneficial π stacking between mesityl groups and vicinal phenanthroline aromatic rings, as evidenced by the X-ray structure of complex **C3** ($[Cu^{I}(Mes\text{-}phen)(\mathbf{L_2})]^{+}$). Electrochemistry of the copper(I) complexes revealed reversible anodic behavior, corresponding to a copper(I) to copper(II) transition. The half wave potentials increase with the steric bulk at the level of the copper(I) ion, reaching a value as high as 1 V vs SCE, with the assistance of ligand induced electronic effects. $\mathbf{L_1}$ and $\mathbf{L_2}$ are further end-capped by a bromo functionality. A Suzuki cross-coupling reaction was directly performed on the complexes, in spite of the handicapping lability of copper(I)−phenanthroline complexes.

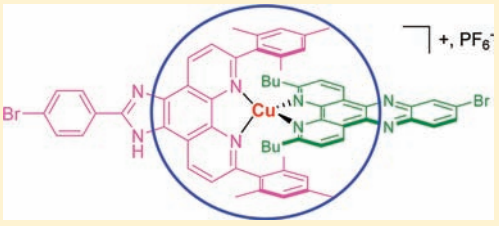

INTRODUCTION

Copper(I)−diimine complexes ($[Cu^{I}(diimine)_2]^{+}$), where the diimine ligand is α-substituted by bulky groups, have attracted much attention since the discovery of their luminescence properties in solution and in the solid state.[1−5] They share with ruthenium−polypyridine complexes several appealing features for solar energy conversion, in particular the existence of a metal to ligand charge transfer transition (MLCT) around 460 nm, which could be formally described as $[Cu^{II}(imine^{\bullet-})(imine)]^{+}$.[3−6] Importantly, the presence of sterically challenging groups in the α position of the coordinating nitrogen atoms is mandatory to observe photoluminescence, since they prevent the flattening distortion of the complex from the Cu^{I} preferred tetrahedral geometry to the formal Cu^{II} square planar arrangement, leading to a very efficient quenching of the excited state. However, the rather low molar extinction coefficient of the MLCT absorption band and the ligand scrambling around Cu(I), preventing the isolation of a stable $[Cu^{I}(imine^{A})(imine^{B})]^{+}$ heteroleptic complex, has put a dramatic curb on the development of

Received: March 28, 2011
Published: October 21, 2011

dx.doi.org/10.1021/ic2006343 | *Inorg. Chem.* 2011, 50, 11309–11322

Chart 1. Structures of the Ligands and Complexes Described in This Study

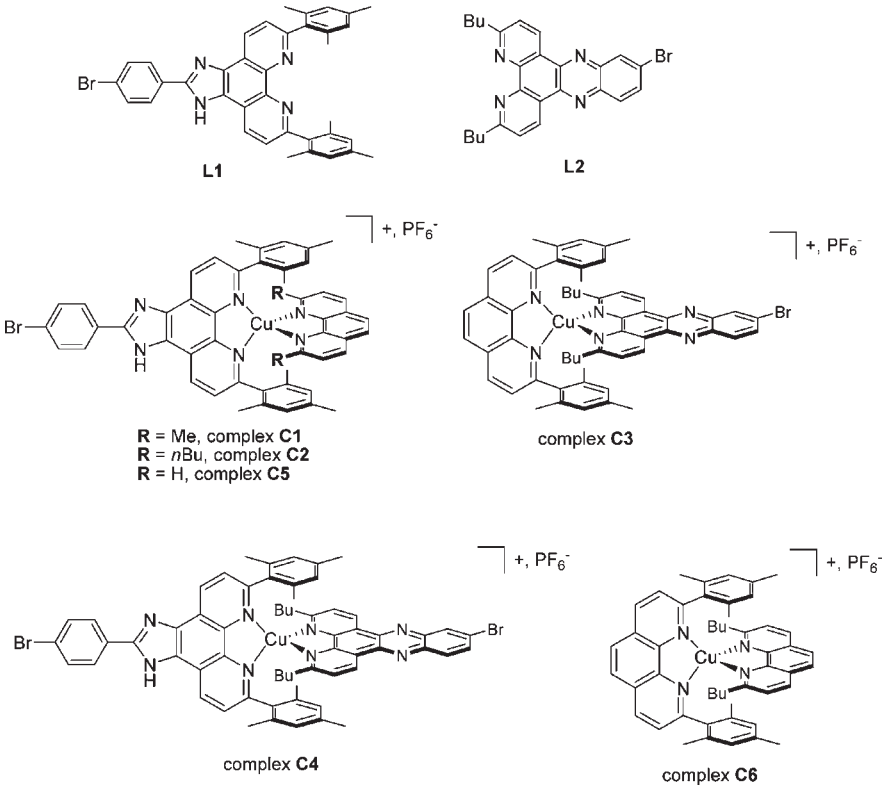

copper-based photosystems. Indeed, the formation of a mere dyad (e.g., with imine^{A} as the electron acceptor and imine^{B} as the electron donor) was strictly impossible, in contrast with the nearly matchless versatility of ruthenium−polypyridine chemistry.[7] However, the ability to prepare heteroleptic diimine copper(I) complexes would be extremely useful for solar energy conversion applications as it would be easier to accurately tune their photophysical and photoredox properties. This is well demonstrated with the abundant use of heteroleptic ruthenium complexes for dye-sensitized solar cells (DSSCs), in which an anchoring ligand (such as 4,4′-dicarboxy-2,2′-bipyridine) is mixed with electron releasing ligands (such as thiocyananto or a bpy substituted with thienyl or oligophenylenethynylene chains) in order to reach the suitable electronic properties to inject electrons in TiO_2 and to harvest the maximum number of photons in the solar spectrum.[8] Second, the preparation of heteroleptic diimine copper(I) complexes opens the route to the development of rodlike multicomponent assemblies, which was not conveniently accessible with the octahedral ruthenium trisbipyridine complex. In 1997, Schmittel and co-workers broke through this barrier, with the HETPHEN concept (where HETPHEN stands for HETeroleptic PHENanthroline copper(I) complexes):[9−12] by grafting very bulky substituents such as mesityl groups (where mesityl stands for 2,4,6-trimethylphenyl) at the 2 and 9 positions of the phenanthroline skeleton, the formation of the corresponding homoleptic complex is prohibited. As a result, numerous impressive and carefully designed copper(I)−phenanthroline supramolecular architectures were isolated and fully characterized.[12−16] A very similar approach has been undertaken using *tert*-butyl instead of mesityl and proved to be very successful.[17] However, in the HETPHEN concept, the mesityl groups borne by phen^{A} are involved in a $\pi-\pi$ interaction with phen^{B}, providing further stability to the molecular scaffold.

At the convergence point of the HETPHEN concept and the luminescence properties of sterically hindered copper(I) complexes lies the possibility to design photosensitive dyads, capable of sustaining photoinduced electron transfer, where phen^{A} behaves as an electron donor and phen^{B} as an acceptor. In addition to the obvious financial advantage of using copper instead of ruthenium, the tetrahedral arrangement of the $[Cu^{I}(phen^{A})(phen^{B})]^{+}$-based arrays is very attractive for the design of linear photosensitive donor−acceptor polyads.

In this work, we describe the synthesis and characterizations of two new, synthetically versatile ligands, $\mathbf{L_1}$ (2,9-dimesityl-2-(4′-bromophenyl)imidazo[4,5-*f*][1,10]phenanthroline) and $\mathbf{L_2}$ (3,6-di-*n*-butyl-11-bromodipyrido[3,2-*a*:2′,3′-*c*]phenazine), and their related heteroleptic copper(I) complexes with phen (1,10-phenanthroline), Me-phen (2,9-dimethyl-1,10-phenanthroline), *n*Bu-phen (2,9-di-*n*-butyl-1,10-phenanthroline), and Mes-phen (2,9-dimesityl-1,10-phenanthroline) (Chart 1). The molecular structures of $\mathbf{L_1}$ and $\mathbf{L_2}$ are inspired by well-known phenanthroline derivatives, phen-imidazole and dppz, respectively (where phen-imidazole is 2-phenylimidazo[4,5-*f*][1,10]phenanthroline and dppz is dipyrido[3,2-*a*:2′,3′-*c*]phenazine), with well documented electronic properties. In particular, dppz has been extensively used in metal-based photosensitive polyads[18−20] and DNA intercalating agents.[21] On the other hand, phen−imidazole derivatives are electron donating in nature and bear a labile proton. With a modest number of new ligands, several original complexes can be synthesized, and the electronic effects of the former on the overall properties of the latter can be explored and constitute the core of this work. Additionally, let us

dx.doi.org/10.1021/ic2006343 |*Inorg. Chem.* 2011, 50, 11309–11322

note that $\mathbf{L_1}$ and $\mathbf{L_2}$ possess a bromo unit, which could be involved in a catalyzed cross-coupling reaction in order to construct larger arrays by chemistry on the complex, a lead that will also be presented in this contribution. The aim of the present work is to provide a detailed analysis of the structural, electrochemical, and spectral properties of the newly synthesized complexes combining experimental and theoretical studies.

EXPERIMENTAL SECTION

General. ^{1}H NMR spectra were recorded on an AMX 400 MHz Bruker spectrometer. Chemical shifts for ^{1}H NMR spectra are referenced relative to residual protium in the deuterated solvent ($CDCl_3$ δ = 7.26 ppm). MALDI-TOF analyses were performed on an Applied Biosystems Voyager DE-STR spectrometer in positive linear mode at a 20 kV acceleration voltage with α-cyano 4-hydroxycinnamic acid (CHCA) as the matrix.

Preparative thin-layer chromatography (preparative TLC) was performed with a Merk Kieselgel 60PF_{254}. Column chromatography was carried out with a Merk 5735 Kieselgel 60F (0.040−0.063 mm mesh). Air sensitive reactions were carried out under argon in dry solvents and glassware. Chemicals were purchased from Aldrich and used as received. Compounds 2,9-dichloro-1,10-phenanthroline-5,6-dioxolane (**2**), 2,9-di-*n*-butyl-1,10-phenanthroline (*n*Bu-phen), 2,9-di-*n*-butyl-1,10-phenanthroline-5,6-dione, and Mes-phen were synthesized using literature procedures.[22]

UV−visible spectra were recorded in analytically pure solvents, with a UV 2501PC Shimadzu spectrophotometer. Luminescence excitation spectra were recorded using a FluoroMax3 (Jobin Yvon Horiba), and emission was corrected for the spectral sensitivity of the instrument. Nanomicrosecond transient absorption experiments were performed using a laser flash photolysis apparatus. Excitation pulses at 460 nm (4 ns, 1 mJ) were provided by a 10-Hz Nd:YAG laser coupled to an OPO (Continuum Panther EX OPO pumped by a Surelite II). The probe light was provided by a pulsed Xe lamp (XBO 150W/CR OFR, OSRAM). Samples were contained in a quartz cell (10 × 10 mm^2 section) at an adjusted concentration ($\sim 10^{-4}$ mol dm^{-3}) to get an OD value of about 1.0 at the pump excitation wavelength. The transmitted light was dispersed by a monochromator (Horiba Jobin-Yvon, iHR320) and analyzed with a photomultiplier (R1477−06, Hamamatsu) coupled to a digital oscilloscope (LeCroy 454, 500 MHz). The experiment was repeated for different wavelengths of the monochromator, and transient spectra were afterward reconstructed. Electrochemistry measurements were performed with an Autolab PGSTAT 302N potentiostat in freshly distilled dichloromethane, with a platinum disk working electrode, a platinum foil counter electrode, and a saturated calomel reference electrode (SCE). Tetra-*n*-butylammonium hexafluorophosphate in dichloromethane (0.1 mol L^{-1}) was used as a supporting electrolyte. All potentials are referenced vs SCE.

Computational Chemistry. The geometries of complexes **C1** to **C6** in the ^{1}A electronic ground state have been optimized at the density functional theory (DFT) level using the PBE-D functional[23] and TZP basis sets[24] for all of the atoms. These calculations are under a C_1 symmetry constraint in a vacuum and have been performed using ADF2010.02 quantum chemistry software.[25] Although PBE-D reproduces the π-stacking structure, it is not good at describing the planarity of the floppy system and tends to make $\mathbf{L_1}$ curved. Therefore, we add several constraints to keep $\mathbf{L_1}$ planar. The theoretical absorption spectra of complexes **C3** and **C6** have been calculated by means of the time-dependent DFT (TD-DFT) method[26] using the B3LYP functional[27] without a solvent effect with the enlarged cc-pVDZ basis sets for the hydrogen, bromide, and second-row atoms[28] and the modified Ahlrichs TZV basis set (7s, 6p, 5d) contracted to [6s, 3p, 3d] for the Cu atom.[29] TD-DFT calculation has been performed using a modified version of the Gaussian 03 quantum chemistry software.[30]

Synthesis. *2,9-Dimesityl-1,10-phenanthroline-5,6-dioxolane (**3**).* In a Schlenk tube fitted with a water condenser, **2** (47 mg, 0.15 mmol), mesitylboronic acid (60 mg, 0.37 mmol), and barium hydroxide (94 mg, 0.55 mmol) were suspended in 5 mL of a 9:1 (v:v) mixture of 1,2-dimethoxyethane (DME) and water, respectively. The setup was thoroughly degassed with argon, and palladium tetrakis triphenylphosphine (20 mg, 0.02 mmol) was quickly added. The mixture was heated to 115 °C and stirred for 16 h, under argon. It was then allowed to cool down to room temperature, and water was added. The suspension was extracted four times with dichloromethane. The organic layers were gathered, dried on sodium sulfate, and evaporated under reduced pressure to afford a brown oil. The latter was purified by chromatography on silica gel, prepared in a 1:1 mixture of hexanes and dichloromethane. The second, bright orange ring was collected, and the solvents were removed by rotary evaporation, yielding **3**. Yield: 63 mg (88%). ^{1}H NMR (300 MHz, $CDCl_3$, 25 °C): δ 8.31 (d, 2H, H_4 and H_7), 7.55 (d, 2H, H_3 and H_8), 6.92 (s, 4H, H_{mes}), 2.31 (s, 6H, $CH_{3,mes}$), 2.12 (s, 12H, $CH_{3,mes}$), 1.92 (s, 6H, $CH_{3,dioxolane}$) ppm. ES-MS (m/z) 489.2 $[M + H]^+$. Anal. for 3.1/2DME·1/2CH_2Cl_2. Found (%): C, 74.01; H, 6.38; N, 4.61. Calcd: C, 74.01; H, 6.65; N, 4.86.

*2,9-Dimesityl-1,10-phenanthroline-5,6-dione (**4**).* Compound **3** (163 mg, 0.33 mmol) was suspended in distilled water (5 mL). TFA (10 mL) was then added dropwise, at room temperature, and the yellow suspension eventually turned bright red. The mixture was then heated at 60 °C for 5 h. The solvents were evaporated, and the brown residue was dissolved in 10 mL of dichloromethane, on top of which was added 10 mL of aqueous sodium hydrogenocarbonate (1.0 mol L^{-1}). After 2 h of vigorous stirring, the mixture turned into a turbid, green-yellow emulsion. The latter was extracted four times with dichloromethane. The organic layers were gathered, washed with brine, dried on sodium sulfate, and evaporated under reduced pressure. The resulting yellow oil was further dried on a vacuum line at room temperature, until a powder eventually appeared. Yield: 130 mg (87%). ^{1}H NMR (300 MHz, $CDCl_3$, 25 °C): δ 8.53 (d, 2H, H_4 and H_7), 7.49 (d, 2H, H_3 and H_8), 6.92 (s, 4H, H_{mes}), 2.30 (s, 6H, $CH_{3,mes}$), 2.14 (s, 12H, $CH_{3,mes}$) ppm. HR-MS (m/z): 893.4067 $[2 M + H]^+$.

*2,9-Dimesityl-1,10-phenanthroline-[a:b]imidazo-(4′-bromophenyl) (**L_1**).* Compound **4** (50 mg, 0.10 mmol), *p*-bromobenzaldehyde (20 mg, 0.11 mmol), and ammonium acetate (170 mg, 2.2 mmol) were dissolved in glacial acetic acid (5 mL) and the mixture was refluxed overnight. After concentration under reduced pressure, water was added to precipitate a beige solid. The latter was subjected to column chromatography on silica, eluting with a gradient of methanol in dichloromethane (0 to 1%). The main yellow ring was collected, and the solvent was removed by rotary evaporation, to afford an off-white powder. Yield: 42 mg (62%). ^{1}H NMR (300 MHz, [D_6] DMSO, 25 °C): δ 13.81 (s, broad, 1H, $H_{imidazole}$), 8.97 (d, 2H, H_4 and H_7), 8.27 (d, 2H, H_{11} and H_{14}), 7.82 (d, 2H, H_{12} and H_{13}), 7.74 (d, 1H, H_3), 7.68 (d, 1H, H_8), 6.95 (s, 4H, H_{mes}), 2.29 (s, 6H, $CH_{3,mes}$), 2.03 (s, 12H, $CH_{3,mes}$) ppm. HR-MS (m/z) 611.1810 $[M+H]^+$. Anal. for $\mathbf{L_1}$·1/2CH_3COOH. Found (%): C, 71.57; H, 5.31; N, 8.38. Calcd: C, 71.14; H, 5.18; N, 8.73.

*2,9-Bis-n-butyl-3′-bromo-dipyrido[3,2-a:2′,3′-c]phenazine (**L_2**).* Compound **5** (91 mg, 0.28 mmol) and 4-bromo-1,2-diaminobenzene (53 mg, 0.28 mmol) were dissolved in 30 mL of ethanol. The mixture was refluxed overnight. After concentration under reduced pressure, the addition of water yielded a brown powder, which was chromatographed on silica, with dichloromethane as an eluent. Yield: 56 mg (62%). ^{1}H NMR (300 MHz, $CDCl_3$, 25 °C): δ 9.50 (m, 2H, H_4 and H_7), 8.53 (d, 1H, H_{13}), 8.20 (d, 1H, H_{11}), 7.95 (dd, 1H, H_{12}), 7.68 (d, 2H, H_3 and H_8), 3.28 (m, 4H, $CH_{2,butyl}$), 1.95 (m, 4H, $CH_{2,butyl}$), 1.55 (m, 4H, $CH_{2,butyl}$), 1.06 (t, 6H, $CH_{3,butyl}$). HR-MS (m/z) 473.1351 $[M]^+$. Anal. for $\mathbf{L_2}$·1/2H_2O. Found (%): C, 64.72; H, 5.38; N, 11.35. Calcd: C, 64.73; H, 5.43; N, 11.61.

dx.doi.org/10.1021/ic2006343 |*Inorg. Chem.* 2011, 50, 11309–11322

General Procedure for the Synthesis of Copper(I) Complexes ***C1*****–*****C6***. $Cu(CH_3CN)_4PF_6$ was dissolved in distilled dichloromethane and thoroughly degassed by a few vacuum/argon cycles. An argon purged solution of mesityl bearing ligand phen^A (**L$_1$** or Mes-phen; 1.0 equivalent) in dichloromethane was then syringed into the former solution, and the mixture was stirred at room temperature. After 5 min, an argon purged solution of ligand phen^B (1.0 equivalent, phen^B = phen, Me-phen, *n*Bu-phen, or **L$_2$**) in dichloromethane was syringed into the yellow mixture. The latter immediately turned deep red and was left to stir for half an hour at room temperature. The solvent was then removed by rotary evaporation. The red residue was eventually purified by chromatography on silica gel. Reactions were all performed at least three times, and yields were all comprised between 75 and 85%. In what follows, H nuclei belonging to phen^B (nonmesityl derivatized) are primed.

C1: obtained with phen^A = **L$_1$**, phen^B = Me-phen. ^{1}H NMR (300 MHz, $CDCl_3$, 25 °C): δ 11.92 (s, 1H, $H^{imidazole}$), 9.45 (d, 1H, H^4 or H^7), 9.36 (d, 1H, H^7 or H^4), 8.34 (d, 2H, H^{11} and H^{14}), 8.22 (d, 2H, $H^{4'}$ and $H^{7'}$), 7.82 (d, 2H, H^{12} and H^{13}), 7.79 (s, 2H, $H^{5'}$ and $H^{6'}$), 7.72 (d, 2H, H^3 and H^8), 7.49 (d, 2H, $H^{3'}$ and $H^{8'}$), 6.11 (s, 2H, $H^{mes,arom}$), 6.02 (s, 2H, $H^{mes,arom}$), 2.21 (s, 6H, $CH_{3,methyl}$), 1.76 (s, 3H, $CH_{3,mes}$), 1.73 (s, 3H, $CH_{3,mes}$), 1.63 (s, 6H, $CH_{3,mes}$), 1.56 (s, 6H, $CH_{3,mes}$). HR-MS (*m*/*z*): 881.2021 $[M\text{-}PF_6]^+$. Anal. for **C1**·CH_3OH. Found (%): C, 58.73; H, 4.28; N, 7.91. Calcd: C, 58.90; H, 4.47; N, 7.93.

C2: obtained with phen^A = **L$_1$**, phen^B = *n*Bu-phen. ^{1}H NMR (300 MHz, $CDCl_3$, 25 °C): δ 11.97 (s, 1H, $H^{imidazole}$), 9.37 (m, 2H, H^4 and H^7), 8.31 (d, 2H, H^{11} and H^{14}), 8.27 (d, 2H, $H^{4'}$ and $H^{7'}$), 7.83 (s, 2H, $H^{5'}$ and $H^{6'}$), 7.78 (d, 2H, H^{12} and H^{13}), 7.65 (d, 2H, H^3 and H^8), 7.48 (d, 2H, $H^{3'}$ and $H^{8'}$), 6.22 (s, 2H, $H^{mes,arom}$), 6.11 (s, 2H, $H^{mes,arom}$), 2.33 (m, 4H, $CH_{2,butyl}$), 1.91 (s, 3H, $CH_{3,mes}$), 1.85 (s, 3H, $CH_{3,mes}$), 1.58 (s, 6H, $CH_{3,mes}$), 1.49 (s, 6H, $CH_{3,mes}$), 1.18 (m, 4H, $CH_{2,butyl}$), 0.80 (m, 4H, $CH_{2,butyl}$), 0.61 (t, 6H, $CH_{3,butyl}$). HR-MS (*m*/*z*): 965.2970 $[M - PF_6]^+$. Anal. for **C2**·1/2CH_3OH. Found (%): C, 61.21; H, 4.85; N, 7.28. Calcd: C, 61.20; H, 5.09; N, 7.26.

C3: obtained with phen^A = Mes-phen, phen^B = **L$_2$**. ^{1}H NMR (300 MHz, $CDCl_3$, 25 °C): δ 9.56 (m, 2H, $H^{4'}$ and $H^{7'}$), 8.76 (d, 2H, H^4 and H^7), 8.60 (d, 1H, $H^{13'}$), 8.28 (m, 3H, H^5, H^6 and $H^{11'}$), 8.04 (dd, 1H, $H^{12'}$), 7.79 (d, 2H, H^3 and H^8), 7.71 (m, 2H, $H^{3'}$ and $H^{8'}$), 6.19 (s, 2H, $H^{mes,arom}$), 6.17 (s, 2H, $H^{mes,arom}$), 2.38 (m, 4H, $CH_{2,butyl}$), 1.72 (s, 6H, $CH_{3,mes}$), 1.62 (s, 6H, $CH_{3,mes}$), 1.60 (s, 6H, $CH_{3,mes}$), 1.24 (m, 4H, $CH_{2,butyl}$), 0.84 (m, 4H, $CH_{2,butyl}$), 0.70 (m, 6H, $CH_{3,butyl}$). HR-MS (*m*/*z*) 953.2801 $[M - PF_6]^+$. Anal. for **C3**·CH_3OH. Found (%): C, 60.63; H, 4.86; N, 7.34. Calcd: C, 60.56; H, 5.08; N, 7.43.

C4: obtained with phen^A = **L$_1$**, phen^B = **L$_2$**. ^{1}H NMR (300 MHz, $CDCl_3$, 25 °C): δ 9.57 (d, 1H, $H^{4'}$ or $H^{7'}$), 9.55 (d, 1H, $H^{7'}$ or $H^{4'}$), 9.45 (d, 2H, H^4 and H^7), 8.64 (d, 1H, $H^{13'}$), 8.38 (d, 2H, H^{11} and H^{14}), 8.31 (d, 1H, $H^{11'}$), 8.08 (dd, 1H, $H^{12'}$), 7.82 (d, 2H, H^3 and H^8), 7.74 (d, 2H, H^{12} and H^{13}), 7.65 (m, 2H, $H^{3'}$ and $H^{8'}$), 6.17 (s, 2H, $H^{mes,arom}$), 6.15 (s, 2H, $H^{mes,arom}$), 2.40 (m, 4H, $CH_{2,butyl}$), 1.72 (s, 6H, $CH_{3,mes}$), 1.62 (s, 6H, $CH_{3,mes}$), 1.60 (s, 6H, $CH_{3,mes}$), 1.25 (m, 4H, $CH_{2,butyl}$), 0.84 (m, 4H, $CH_{2,butyl}$), 0.64 (m, 6H, $CH_{3,butyl}$). HR-MS (*m*/*z*): 1145.2266 $[M - PF6]^+$. Anal. for **C4**·2CH_3OH. Found (%): C, 57.43; H, 4.56; N, 8.02. Calcd: C, 57.51; H, 4.75; N, 8.25.

C5: obtained with phen^A = **L$_1$**, phen^B = Phen. Data for complex **C5**: ^{1}H NMR (300 MHz, $CDCl_3$, 25 °C): δ 9.36 (d, 2H, H^4 and H^7), 8.50 (d, 2H, $H^{2'}$ and $H^{9'}$), 8.39 (d, 2H, $H^{4'}$ and $H^{7'}$), 8.32 (d, 2H, H^{11} and H^{14}), 7.86 (s, 2H, $H^{5'}$ and $H^{6'}$), 7.82 (d, 2H, H^{12} and H^{13}), 7.70 (m, 4H, H^3, H^8, $H^{3'}$ and $H^{8'}$), 5.88 (s, 4H, $H^{mes,arom}$), 1.70 (s, 12H, $CH_{3,mes}$), 1.53 (s, 6H, $CH_{3,mes}$). HR-MS (*m*/*z*): 853.1721 $[M\text{-}PF_6]^+$. Anal. for **C5**·CH_3OH. Found (%): C, 58.15; H, 4.17; N, 7.84. Calcd.: C, 58.17; H, 4.20; N, 8.14.

C6: obtained with phen^A = Mes-phen, phen^B = *n*Bu-phen. ^{1}H NMR (300 MHz, $CDCl_3$, 25 °C): δ 8.70 (d, 2H, H^4 and H^7), 8.31 (d, 2H, $H^{4'}$ and $H^{7'}$), 8.24 (s, 2H, H^5 and H^6), 7.85 (s, 2H, $H^{5'}$ and $H^{6'}$), 7.76 (d, 2H, H^3 and H^8), 7.51 (d, 2H, $H^{3'}$ and $H^{8'}$), 6.20 (s, 4H, $H^{mes,arom}$), 2.31 (m, 4H, $CH_{2,butyl}$), 1.91 (s, 6H, $CH_{3,mes}$), 1.54 (s, 12H, $CH_{3,mes}$), 1.16 (m, 4H, $CH_{2,butyl}$), 0.81 (m, 4H, $CH_{2,butyl}$), 0.67 (m, 6H, $CH_{3,butyl}$). HR-MS (*m*/*z*): 771.3489 $[M - PF_6]^+$. Anal. for **C6**·CH_3OH·H_2O. Found (%): C, 63.31; H, 6.08; N, 5.44. Calcd: C, 63.31; H, 6.04; N, 5.79.

Complex ***C7***. In a Schlenk tube fitted with a water condenser, **C2** (27 mg, 0.024 mmol) and *p*-methoxyphenyl boronic acid (19 mg, 0.13 mmol) were dissolved in 4 mL of a 9:1 (v/v) mixture of 1,2-dimethoxyethane (DME) and water, respectively. Barium hydroxide (50 mg, 0.29 mmol) was then added. The setup was thoroughly degassed with argon, and palladium tetrakis triphenylphosphine (3 mg, 0.003 mmol) was quickly added. The mixture was heated to 110 °C and stirred for 16 h, under argon. It was then allowed to cool down to room temperature, and water was added. The orange suspension was extracted three times with dichloromethane. The organic layers were gathered, dried on sodium sulfate, and evaporated under reduced pressure. The product was purified by column chromatography on silica gel and eluted with a gradient of methanol in dichloromethane (from 2% to 10%) to yield a red powder. Yield: 9 mg, 34%. ^{1}H NMR (300 MHz, $CDCl_3$, 25 °C): δ 15.30 (s broad, 1H, $H^{imidazole}$), 10.46 (s broad, 1H, H^4 or H^7), 9.40 (d, 1H, H^7 or H^4), 8.88 (d, 2H, H^{11} and H^{14}), 8.22 (d, 2H, $H^{4'}$ and $H^{7'}$), 7.77 (m, 6H, $H^{5'}$, $H^{6'}$, H^3, H^8, H^{12} and H^{13}), 7.63 (d, 2H, H^{15} and H^{18}), 7.46 (d, 2H, $H^{3'}$ and $H^{8'}$), 7.00 (d, 2H, H^{16} and H^{17}), 6.20 (s, 2H, $H^{mes,arom}$), 6.11 (s, 2H, $H^{mes,arom}$), 3.88 (s, 3H, OCH_3), 2.35 (m, 4H, $CH_{2,butyl}$), 1.90 (s, 3H, $CH_{3,mes}$), 1.86 (s, 3H, $CH_{3,mes}$), 1.57 (s, 6H, $CH_{3,mes}$), 1.49 (s, 6H, $CH_{3,mes}$), 1.18 (m, 4H, $CH_{2,butyl}$), 0.82 (m, 4H, $CH_{2,butyl}$), 0.62 (t, 6H, $CH_{3,butyl}$). HR-MS (*m*/*z*): 993.4243 $[M - PF_6]^+$.

Complex ***C8***. In a Schlenk tube fitted with a water condenser, **C3** (25 mg, 0.022 mmol) and *p*-methoxyphenyl boronic acid (18 mg, 0.12 mmol) were dissolved in 2 mL of a 9:1 (v/v) mixture of 1,2-dimethoxyethane (DME) and water, respectively. Barium hydroxide (39 mg, 0.23 mmol) was then added. The setup was thoroughly degassed with argon, and palladium tetrakis triphenylphosphine (5 mg, 0.004 mmol) was quickly added. The mixture was heated to 110 °C and stirred for 16 h, under argon. It was then allowed to cool down to room temperature, and water was added. The orange suspension was extracted three times with dichloromethane. The organic layers were gathered, dried on sodium sulfate, and evaporated under reduced pressure. The product was purified by column chromatography on silica gel and prepared with CH_2Cl_2/CH_3OH (= 94:6) to yield a red powder.

Yield: 21 mg, 84%. ^{1}H NMR (300 MHz, $CDCl_3$, 25 °C): δ 9.59 (2d, 2H, $H^{4'}$ and $H^{7'}$), 8.76(d, 2H, H^4 and H^7), 8.55 (d, 1H, $H^{13'}$), 8.43 (d, 1H, $H^{11'}$), 8.28 (m, 3H, H^5, H^6 and $H^{12'}$), 7.86 (d, 2H, $H^{14'}$ and $H^{17'}$), 7.79 (d, 2H, H^3 and H^8), 7.68 (2d, 2H, $H^{3'}$ and $H^{8'}$), 7.13 (d, 2H, $H^{15'}$ and $H^{16'}$), 6.19 (s, 4H, $H^{mes,arom}$), 3.94 (s, 3H, OCH_3), 2.39 (m, 4H, $CH_{2,butyl}$), 1.74 (s, 6H, $CH_{3,mes}$), 1.62 (s, 12H, $CH_{3,mes}$), 1,25 (m, 4H, $CH_{2,butyl}$), 0.85 (m, 4H, $CH_{2,butyl}$), 0.70 (m, 6H, $CH_{3,butyl}$). HR-MS (*m*/*z*): 979.4152 $[M\text{-}PF_6]^+$.

Crystal Structure Data for $C_{56}H_{53}BrCuN_6 \cdot PF_6 \cdot (ClCH_3)_{0.629}$. Structure data are as follows: M_w = 1130.2, colorless block, 0.4 × 0.2 × 0.15 mm^3, triclinic, $P\bar{1}$, a = 13.6027(6) Å, b = 14.2161(14) Å, c = 15.4400(5) Å, α = 73.945(6)°, β = 83.606(6)°, γ = 85.364(7)°, V = 2847.5(3) Å^3, Z = 2, D_x = 1.318 g cm^{-3}, μ = 1.2 mm^{-1}. A total of 82 229 reflections were measured on a Nonius-Kappa CCD diffractometer (graphite monochromator, λ = 0.71073 Å) up to a resolution of $(\sin\theta/\lambda)_{max}$ = 0.66 Å^{-1} at 100 K. A total of 13 612 reflections were unique (R_{int} = 0.10). The structure was solved using the charge flipping algorithm[31] implemented in the Superflip program[32] and refined with the JANA2006 program[33] against F^2 for all reflections. A disorder in the **L$_2$** moiety, i.e., the superposition of the two regioisomers, was correctly modeled using a rigid body approach. However, the solvent molecules occupying the large void (>200 Å) could not be determined; only two chloromethane solvent molecules with a partial occupancy ratio were identified. Obviously, the solvent molecules are disordered correlatively with the **L$_2$** moiety.

Scheme 1. Synthesis of Ligands L_1 and L_2[a]

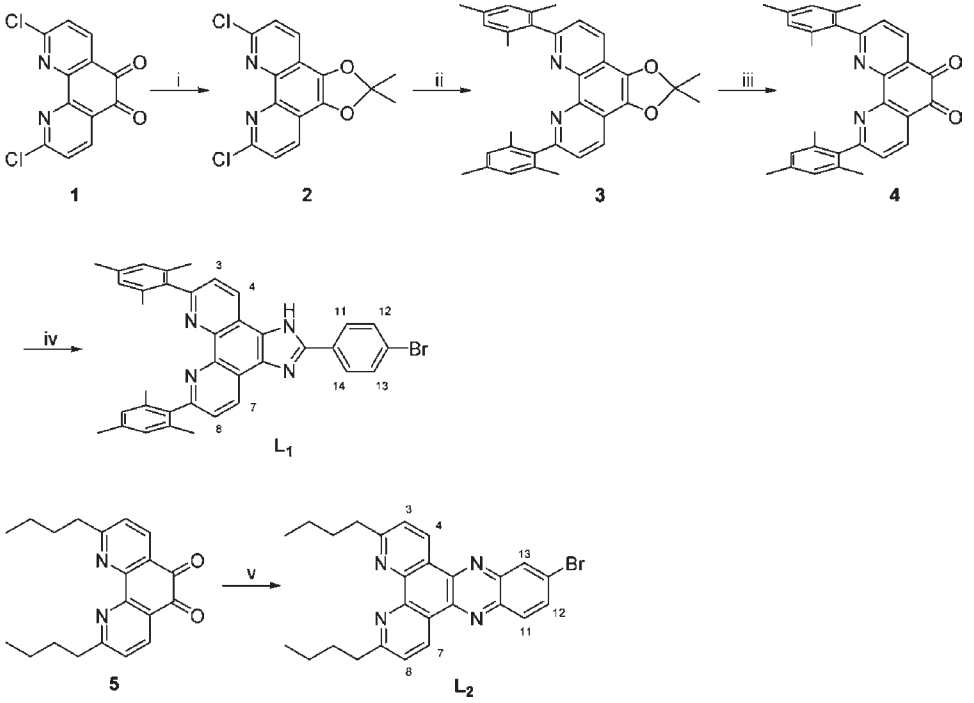

[a] i: 2-nitropropane, Na_2CO_3, reflux under argon; yield: 91%. ii: dimethylethyleneglycol/H_2O (10/1), $Ba(OH)_2$, mesityl boronic acid, $Pd(PPh_3)_4$, reflux under argon; yield: 88%. iii: TFA, H_2O, CH_2Cl_2, R.T.; yield: 87%. iv: 4-bromobenzaldehyde, NH_4OAc (20 eqv.), glacial acetic acid, reflux; yield: 62%. v: 4-bromo-1,2-phenylenediamine, ethanol at reflux; yield: 62%.

Non-hydrogen atoms were refined with anisotropic displacement parameters. All H atoms were introduced in geometrically optimized positions and refined with a riding model, except for methyl group H atoms, the positions of wich were refined under constraints. Altogether, 674 parameters were refined. R_1/wR_2 [$I \geq 2\sigma(I)$] = 0.1124/0.2534. R_1/wR_2 [all reflections] = 0.1625/0.2675, S = 3.25. Residual electron density is rather large (between 4.2 and −4.9 $e^-Å^{-3}$), due to the disorder and the unsolved solvent void.

CCDC 818959 contains the supplementary crystallographic data for this paper. These data can be obtained free of charge from The Cambridge Crystallographic Data Centre via www.ccdc.cam.ac.uk/data_request/cif.

Synthesis. The syntheses of ligands L_1 and L_2 require two very similar building blocks: 2,9-dimesityl- and 2,9-di-*n*-butyl-1,10-phenanthroline-5,6-dione, **4** and **5**, respectively (Scheme 1). The synthesis of the latter has been previously reported[34] and consists of the classic chemical oxidation of *n*-Bu-phen[35] in a mixture of sulphuric and nitric acid with sodium bromide. These rather harsh conditions require a cautious "every second control" of the reaction medium (temperature, stirring velocity, etc.). Under the same conditions, Mes-phen was irremediably damaged, and no traces of **4** were ever detected. We therefore explored a different approach, proposed by Sauvage and co-workers,[22] relying on Suzuki's palladium catalyzed cross coupling reaction. Dione **1** was obtained following literature procedures.[22,36] First of all, **1** was protected in the presence of 2-nitropropane in a basic aqueous medium; the resulting ketal was reacted with mesityl boronic acid, in the presence of barium hydroxide and tetrakis triphenylphosphine palladium(0). The protection step appeared to be mandatory to avoid degradation of the phendione core into a fluorenone derivative, under the Suzuki reaction conditions. The bis-functionalized product **3** was obtained in 88% yield, after purification by chromatography. Subsequent deprotection in TFA afforded dione **4**, which was reacted with 4-bromo-benzaldehyde in acetic acid at reflux, in the presence of excess ammonium acetate, yielding ligand L_1.[37]

^{1}H NMR confirmed the molecular structures of both L_1 and L_2. As regards L_1, it is worth noticing the presence of a broad, very unshielded signal at 13.81 ppm, assigned to the slightly acidic proton borne by the imidazole ring. Furthermore, a singlet is observed at 6.95 ppm, characteristic of the four hydrogen nuclei from the two mesityl groups. The signals corresponding to the phenanthroline moiety (H^3, H^4, H^7, and H^8) deserve, however, a comment. In Figure S1 (Supporting Information), H^3 and H^8 are not chemically equivalent, being displayed as two separate doublets. The presence of an impurity, like an oxazole derivative, traditionally obtained as a side product in Steck and Day's synthetic protocol,[37] can be ruled out since HR-MS and microanalysis are both in agreement with the proposed structure for L_1. Such a peculiar behavior could be explained by the asymmetry of the imidazole ring in which one nitrogen is protonated and the other is free. Indeed, in the presence of a strong acid (trifluoroacetic acid) or an organic base (triethylamine), the two doublets actually merge, giving rise to the spectrum of a fully C_{2v} symmetric molecule (see Figure S1). $H^{imidazole}$ might somehow induce some asymmetry in the system, resulting in nonequivalent H^3 and H^8. The effect is milder on H^4 and H^7, yet the corresponding doublet is slightly broader, with a full width at half-maximum of 2.9 vs 2.3 Hz for H^3 and H^8. Despite this puzzling feature, the spectra of L_1 and L_2 fall within the same range of chemical shifts as their nonsubstituted counterparts, 2-(4-bromophenyl)imidazo[4,5-f]-1,10-phenanthroline[38,39] (see Figure S2, Supporting Information) and 11-bromodipyrido[3,2-*a*:2′,3′-*c*]phenazine,[20] respectively, highlighting the feeble electronic interaction between the phenanthroline core and the bulky groups grafted on positions 2 and 9.

The copper(I) complexes were synthesized in distilled, argon-purged dichloromethane (Scheme 2). In the HETPHEN concept, the idea is to place highly bulky phen^A (Mes-phen or parent L_1) opposite to a less sterically challenged phenanthroline ligand (phen^B) in the presence of copper(I) in solution. The steric bulkiness of mesityl pendant groups prevents the formation of homoleptic species. Tetrakis(acetonitrile)

Scheme 2. Synthesis of Copper(I) Complexes C1−C5

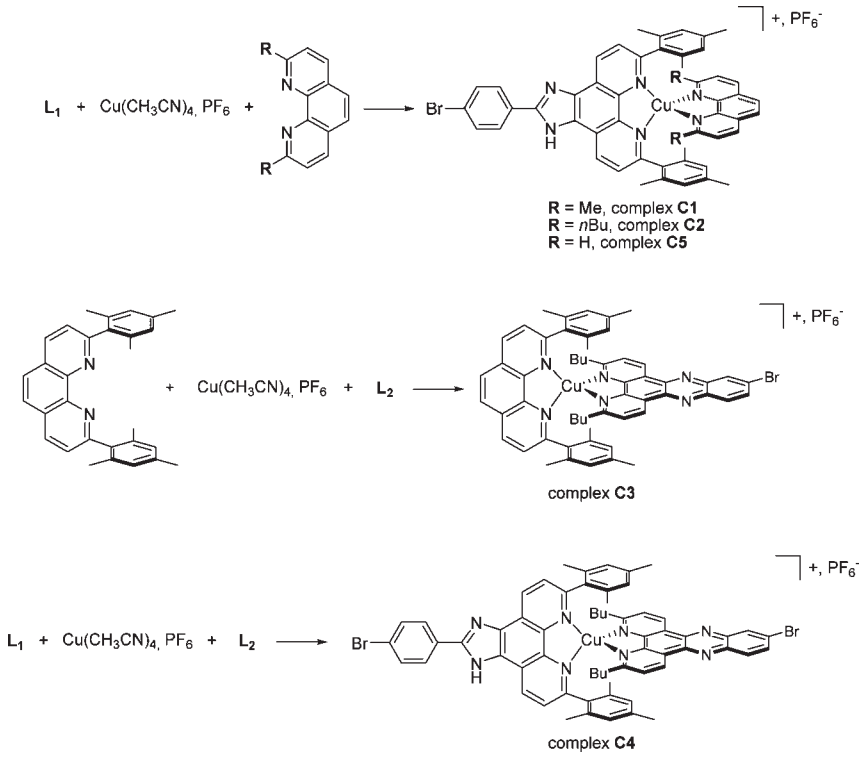

copper(I) hexafluorophosphate $[Cu^{I}(CH_3CN)_4]PF_6$[40] was first dissolved, and one equivalent of ligand $\mathbf{L_1}$ or Mes-phen was added, under argon. The solution turned yellow at once, upon formation of the solvato complexes $[Cu^{I}(\text{Mes-phen})(CH_3CN)]^+$ or $[Cu^{I}(\mathbf{L_1})(CH_3CN)]^+$. Once the complementary ligand phen^{B} (phen^{B} = phen, Me-phen, *n*Bu-phen, or $\mathbf{L_2}$) was added to the mixture, the color quickly turned deep red, evidencing the formation of a copper complex bearing two phenanthroline ligands. Complexes $[Cu^{I}(\mathbf{L_1})(\text{phen}^{B})](PF_6)$ (complex **C1** if phen^{B} = Me-phen, complex **C2** if phen^{B} = *n*Bu-phen, complex **C4** if phen^{B} = $\mathbf{L_2}$ and complex **C5** if phen^{B} = phen) and $[Cu^{I}(\text{Mes-phen})(\mathbf{L_2})](PF_6)$ (complex **C3**) were chromatographed on silica gel and characterized by ^{1}H NMR, HR-MS, and elemental analysis, evidencing the unambiguous formation of pure heteroleptic copper(I) complexes. Complex **C6** ($[Cu^{I}(\text{Mes-phen})(n\text{Bu-phen})](PF_6)$ was synthesized too, being a convenient and simple model of the coordination cages for **C1**−**C5**. ^{1}H NMR spectra revealed again that some hydrogen nuclei are nonequivalent, all the singlets describing mesityl aromatic and aliphatic protons being for instance split into two signals. In presence of traces of water, the spectrum of a fully symmetrical molecule was obtained, along with the disappearance of the imidazole signal, supporting that $H^{\text{imidazole}}$ is playing a crucial role in the symmetry of the complexes **C1**, **C2**, and **C4**. In addition to this, an overall slight downfield shift for most signals was observed, due to the presence of copper in the phenanthroline cavity. On the other hand, $\pi-\pi$ interactions between the mesityl groups of $\mathbf{L_1}$ (or Mes-phen) and the phenanthroline core of each ligand phen^{B} lead to the upfield shift of the aromatic mesityl H signal (see Figure S3, Supporting Information).

RESULTS

X-Ray Structure vs DFT Optimized Structures. Slow diffusion of cyclohexane into a solution of **C3** in dichloromethane

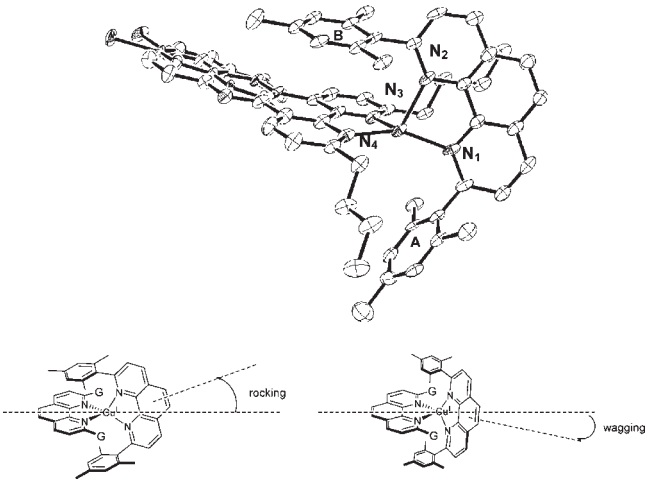

Figure 1. Top: ORTEP view of complex **C3**. Ellipsoids are drawn at the 50% probability level. Bottom: definitions of the rocking and wagging angles.

afforded crystals that were suitable for a structure resolution by X-ray diffraction at 100 K. The ORTEP view is given in Figure 1, and the obtained structure is featured in the Supporting Information (Figure S4, H atoms, two chloromethane solvent molecules, and counterion PF_6^- have been removed for clarity). The hypothesized geometry of the metal center is confirmed, namely, a very distorted tetrahedral symmetry, with a copper(I) ion surrounded by four coordinating nitrogen atoms. Relevant distances and angles are given in Table 1. The structure symmetry is triclinic $P\bar{1}$. Although a rather clear picture of the coordination

dx.doi.org/10.1021/ic2006343 |*Inorg. Chem.* 2011, 50, 11309–11322

Table 1. Selected Bond Lengths (in Å) and Bond Angles (in deg) of Complexes C1 to C6 (Numbering of the Atoms According to the Structures Depicted in Figure 2)[a]

geometrical parameters		C1	C2	C3	C4	C5	C6
$Cu-N_{phen^B}$	$Cu-N_4$	2.003	2.005	2.003	1.999	1.996	2.011
				2.009			
	$Cu-N_3$	2.028	2.060	2.075	2.072	2.025	2.075
				2.115			
$Cu-N_{phen^A}$	$Cu-N_1$	2.020	2.014	2.008	1.999	2.006	2.017
				2.004			
	$Cu-N_2$	2.031	2.057	2.075	2.068	2.023	2.071
				2.124			
bite angles $N_{phen^B}-Cu-N_{phen^A}$	N_3-Cu-N_4	83.35	82.65	82.15	82.24	83.27	82.36
				81.45			
bite angles $N_{phen^A}-Cu-N_{phen^B}$	N_1-Cu-N_2	81.88	82.32	82.26	82.49	82.12	81.96
				81.98			
$N_{phen^B}-Cu-N_{phen^A}$	N_3-Cu-N_1	131.84	124.87	124.55	124.52	133.08	124.32
				123.38			
	N_2-Cu-N_3	109.10	100.42	97.31	96.75	109.35	98.68
				95.53			
	N_1-Cu-N_4	127.58	142.04	144.47	144.67	123.85	143.09
				147.18			
	N_2-Cu-N_4	127.58	121.34	120.47	120.10	131.24	122.21
				119.68			

[a] Bold cells: experimental corresponding values measured from the X-ray structure of complex **C3** shown in Figure 1. $Phen^A$ and $Phen^B$ refer respectively to mesityl and non-mesityl derivatized ligands.

sphere of copper(I) is given by the X-ray structure, the $\mathbf{L_2}$ moiety is subjected to a very disordered environment, as evidenced in Figure 1. Indeed, the bromine atom, which is end-capping the phenazine appendix of $\mathbf{L_2}$, entails the existence of two regioisomers for **C3**, **C3a** and **C3b**. Unexpectedly though, both molecules crystallize almost the same way, in identical crystallographic positions at the level of the {Cu(Mes-Phen)(*n*Bu-Phen)} moiety; the structures of the isomers start to slightly diverge along the phenazine spacer axis. The complex diffraction pattern could nevertheless be well fitted considering a ratio of 3:7 for **C3a**/**C3b**, with a very satisfying R factor, vouching for the accuracy of the structure. This rather peculiar behavior has been previously observed for the complex $[ReCl(CO)_3(dppzBr)]^{2+}$, where dppzBr is same as $\mathbf{L_2}$ but devoid of *n*-butyl chains.[20] Indeed, the singly brominated dppz ligand appeared nonetheless symmetrical, as if doubly substituted, in the structure. In our case, we present in Figure 1 the overlay of the structures of both regioisomers, which do not exactly coincide at the level of the brominated end but perfectly match at the level of the copper coordination cage. Let us add that part of the remaining disorder afflicting the structure is due to the fact that solvent molecules for **C3a** and **C3b** do not occupy the same crystallographic positions.

To sum up, Cu−N bond lengths are typical of copper(I) phenanthroline complexes,[35,38,39,41,42] each ligand being coordinated to copper(I) through two nonequivalent Cu−N bonds ($Cu-N_1$ = 2.004 Å, $Cu-N_2$ = 2.124 Å, $Cu-N_3$ = 2.009 Å, $Cu-N_4$ = 2.115 Å). N−Cu−N bite angles are very similar (81.98° and 81.45°), owing to the rigidity of both phenanthroline derivatized ligands Mes-phen and $\mathbf{L_2}$. Most importantly, an obvious π stacking is evidenced between just one mesityl substituent of ligand Mes-phen (label B in Figure 1) and the adjacent $\mathbf{L_2}$ phenanthroline, with a typical distance of ca. 3.45 Å.[38,39] This

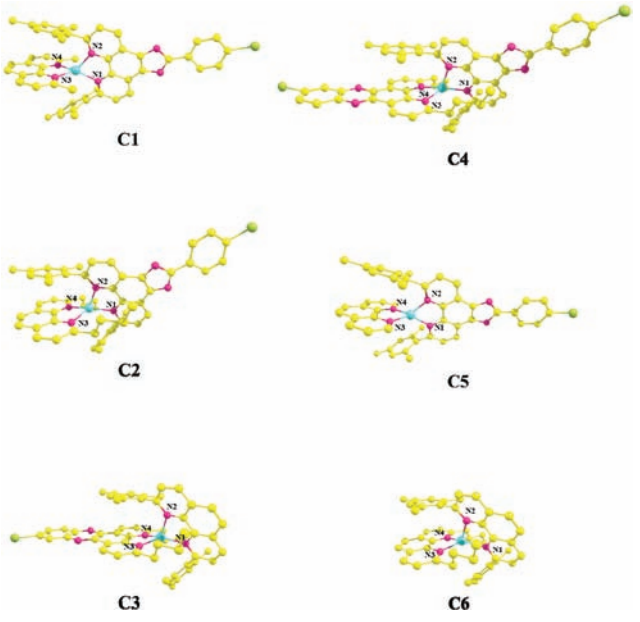

Figure 2. DFT/PBE-D optimized structures of complexes **C1** to **C6**.

entails a strong deviation from the ideal tetrahedral geometry at the copper(I) center toward a heavily distorted trigonal pyramid.[2] As a consequence, the other mesityl substituent (label A in Figure 1) is unable to interact with $\mathbf{L_2}$, being too remote from the latter. This explains as well why the dihedral angles between the mesityl groups and the phenanthroline plane of Mes-phen are significantly different (64.11° for the more constrained mesityl group vs 72.97° for the other). Overall, ligand Mes-phen has

dx.doi.org/10.1021/ic2006343 |*Inorg. Chem.* 2011, 50, 11309–11322

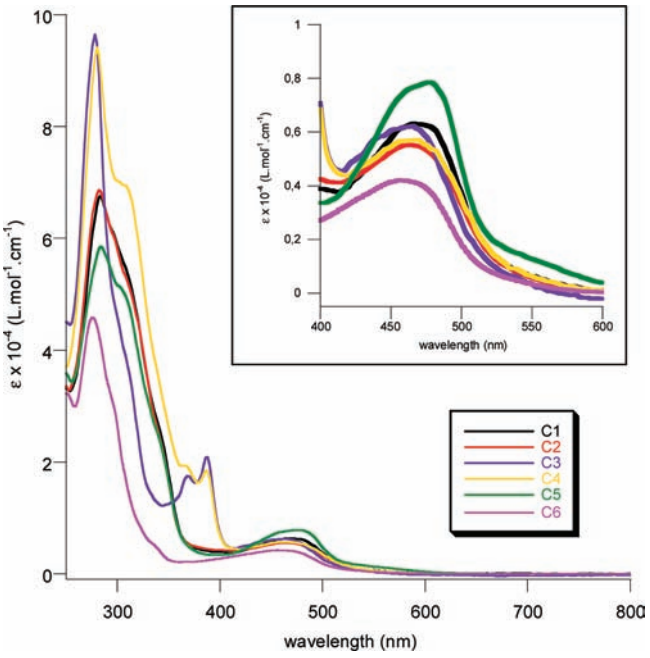

Figure 3. Electronic absorption spectra of complexes **C1**−**C6** in dichloromethane. Inset: magnification of the 400−600 nm domain.

Table 2. Spectroscopic and Electrochemical Data for Complexes C1−C6 and Reference $[Cu^{I}(Me\text{-}phen)_2]^{+a}$

complex	λ_{MLCT}/nm (ε/L mol^{-1} cm^{-1})	$E_{1/2}$ (V) vs SCE ($\Delta E = E_{pa} - E_{pc}$, mV)^{b}
C1	468 (6300)	0.87 (95)
C2	463 (5500)	0.94 (105)
C3	465 (6300)	−1.09 (95), 1.06 (85)
C4	467 (5700)	−1.03 (80), 1.05 (140)
C5	476 (7850)	0.71 (95)
C6	458 (4250)	0.99 (140)
$[Cu^{I}(Me\text{-}phen)_2]^{+}$	455 (7950)^{c}	0.83 (110)

[a] All measurements performed in distilled dichloromethane at room temperature. [b] Recorded in dichloromethane/TBAP 0.1 M with a platinum disk as the working electrode and SCE as a reference. [c] See ref 47.

"rocked and wagged away" from the ideal D_{2d} symmetry. This is in full agreement with the structures of previously published complexes of the type $[Cu^{I}(Mes\text{-}phen)(Phen')]^{+}$,[11,13,16,39] although in the latter case Phen′ did not bear any bulky substituents at the 2 and 9 positions and was not substituted with fused imidazole or phenazine.

The structures of complexes **C1**−**C6** have been scrutinized using DFT/PBE-D/TZP calculations. Selected theoretical bond lengths and bond angles of complexes **C1**−**C6** are reported in Table 1 together with some experimental X-ray data of complex **C3** for comparison. The optimized structures are represented in Figure 2.

The optimized geometries compare rather well with the X-ray data reported in Table 1 for complex **C3** and with the structures of similar complexes of Cu(I). The four main Cu−N coordination bond distances vary between 2.00 and 2.08 Å, slightly shorter than the experimental values which span between 2.004 and 2.124 Å. The calculated Cu-heteroleptic ligands' bond angles are very close to the experimental angles of 81.45° and 81.98°. The structures of **C2**, **C3**, **C4**, and **C6**, which have *n*-Bu-phen ligands, are very similar. They have two shorter Cu−N bonds (2.00−2.02 Å) and longer Cu−N bonds (2.06−2.08 Å), and the angles of N_1-Cu-N_4 are large (142−145°). On the other hand, in **C1** and **C5** complexes, which do not contain *n*-Bu-phen ligands, all four Cu−N bonds are very close (2.00−2.03 Å), and the N_1-Cu-N_4 angles amount to 128° and 124°, respectively. These differences may be attributed to the steric hindrance of *n*-Bu and π-stacking mesityl groups toward one side of the *n*-Bu-phen ligand. Cartesian coordinates of these structures are shown in Table S1 (Supporting Information).

UV−Visible Absorbance Spectroscopy and TD-DFT Absorption Spectra. The electronic absorption spectra of complexes **C1**−**C6** are given in Figure 3, and corresponding data are gathered in Table 2. All complexes displayed a set of intense bands in the UV region that were all assigned to ligand-centered $\pi-\pi^*$ transitions.

In the visible domain, all spectra are dominated by the expected copper(I) to phen MLCT, around 460 nm, which corresponds to the promotion of one electron from the copper(I) center toward a phen centered π^* orbital, yielding a charge separated state that can be formulated Cu^{II}-(phen$^{\bullet-}$). With the exception of complex **C5**, the MLCT energy of complexes **C1**−**C4** and **C6** is only slightly dependent on the structure. Nevertheless, the absorption maximum of **C1** is slightly but sensibly red-shifted compared to **C2**, **C3**, and **C4**. The reason lies in the steric hindrance within the coordination cage around the copper(I) cation. Indeed, it has been reported that the bulkier the substituents, the more rigid the coordination cage, and the higher the energy of the MLCT.[42,43] There are exceptions to this simple rule, in particular for $[Cu^{I}(2,9\text{-diphenyl-}1,10\text{-phenanthroline})_2]^{+}$, since π stacking of the phenyl substituents with the vicinal phenanthroline may entail the $D_{2d} \rightarrow D_2$ transition.[2] For complexes **C1**−**C4** and **C6**, alkyl chains are opposed to mesityl groups, creating a rather bulky environment within the coordination sphere of copper(I); the fact that the methyl group is less sterically demanding than the *n*-butyl chain could account for the slight red-shift of the MLCT in **C1**, compared to **C2**−**C4** and **C6**.[43] This is even more blatant in the case of complex **C5**, where the encumbered 2,9-dimesityl-phenanthroline type ligand $\mathbf{L_1}$ is facing plain phenanthroline. Additionally, the MLCT of **C5** exhibits a broad shoulder around 550 nm, which is a diagnostic band for stronger D_2 deformation, likely due to π stacking between phenanthroline and the mesityl groups.[2,3,41] This transition is nevertheless rather weak when compared to other complexes, especially those built on 2,9-diphenyl phenanthroline (R = phenyl). For $\mathbf{L_1}$ (and Mes-phen), the presence of the mesityl groups greatly increases the steric hindrance of the coordination cage, thus limiting the extent of D_{2d} to D_2 deformation.

Interestingly, the energies of the MLCT in complex **C6** and homoleptic $[Cu^{I}(Me\text{-}phen)_2]^{+}$ are almost identical, being blue-shifted by 5 to 10 nm when compared to **C1**−**C4**. The coordination spheres of **C1**−**C4** and **C6** are very similar (which is supported by DFT calculations), and the rigidity of the copper−phenanthroline core cannot therefore be invoked here to rationalize this experimental fact. On the other hand, the conjugation of $\mathbf{L_1}$ and/or $\mathbf{L_2}$ likely entails a stabilization of the MLCT state; the effect remains however rather weak. Let us add that heteroleptic copper complexes display usually a sensibly lower energy MLCT than their homoleptic counterparts (about

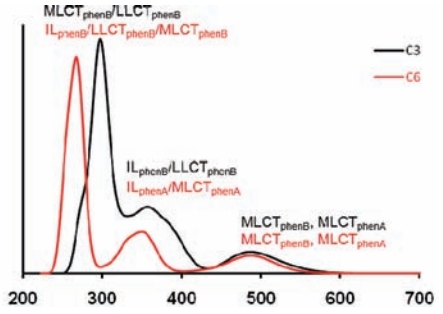

Figure 4. TD-DFT Theoretical Absorption Spectra of Complexes **C3** and **C6**.

10 nm). The existence of a dipole taking its origin in the asymmetry of complexes **C1**−**C5** could as well be held responsible for stabilizing the MLCT, this dipole being of a lesser intensity for **C6**. Additionally, the $\pi-\pi$ interaction between the mesityl groups and the adjacent phenanthroline might as well account for the observed red shift of the MLCT for **C1**−**C4** (and marginally **C6**) compared to $[Cu^{I}(n\text{Bu-phen})_2]^+$.

A greater delocalization of the π electrons on conjugated $\mathbf{L_2}$ may explain the slight red-shift of the MLCT of complex **C4** compared to **C2** confirmed by theory (see Table 2). The energy change here is very small though. Much larger shifts to longer wavelengths have been observed for phenyl- or phenylalkynyl-substituted phenanthrolines.[2,44] But in the famous case of dppz and complexes thereof, it has been demonstrated that the fused phenazine and bipyridine moieties behave a lot like independent units, from the spectroscopic and electrochemical points of view.[45,46] It is therefore not surprising that the MLCT energy is only marginally affected by the presence of the phenazine appendix, just like ruthenium complexes are.

The extinction coefficient of the MLCT depends as well on the structure of the coordination sphere caging the copper(I) cation. Since the latter remains roughly the same all along the series **C1**−**C4** and **C6**, the values of ε are all held within a narrow frame, ranging from 4250 to 6300 M^{-1} cm^{-1}, in good agreement with previously published data.[1,3,4] It is worth mentioning here that poorer ε are not uncommon; values as low as 3000 M^{-1} cm^{-1} were obtained for complex $[Cu^{I}$(2,9-diphenyl-1,10-phenanthroline$)_2]^+$. This was mainly due to a counterproductive effect of the electron delocalization on the transition dipole.[2,47] As evoked above, mesityl groups are much more sterically challenging than mere phenyl rings, and the torsion angle between the phenanthroline and the mesityl planes dramatically decreases the eventual interaction of their π systems. This is in agreement with the similar spectral features measured for $\mathbf{L_1}$ and its unsubstituted counterpart 2-(parabromo phenylimidazo)-[4,5-*f*][1,10]phenanthroline. Yet, the extinction coefficient of the MLCT is significantly smaller for **C6** than for **C1**−**C4**. This might be due to feeble delocalization of the electrons on the mesityl rings, lessening the transition dipole. This effect would then be counterbalanced by the strong delocalization of the electrons on the π systems of $\mathbf{L_1}$ or $\mathbf{L_2}$ for **C1**−**C5**. Let us finish by saying that the spectra of all complexes remain unaltered in aerated dichloromethane or acetonitrile solutions for several days, and even when exposed to air moisture. The stability of these species could be the result of the favorable $\pi-\pi$ stacking between mesityl aromatic groups and the vicinal phenanthroline ligand phen.

Table 3. TD-DFT Wavelengths (in nm) to the Low-Lying Singlet Excited States of Complexes C3 and C6 and Associated Oscillator Strengths Greater than 0.02[a]

complex	state	ΔE (nm)	f
C3			
	MLCTphenB	522	0.02
	MLCTphenA	494	0.04
	MLCTphenA	482	0.02
	MLCTphenB	464	0.03
	LLCTphenB/ILphenB	393	0.06
	LLCTphenB/ILphenB	384	0.05
	LLCTphenB	378	0.04
	ILphenB	372	0.02
	LLCTphenB/ILphenB	362	0.04
	ILphenB/LLCTphenB	357	0.10
	MLCTphenA/ILphenB	349	0.02
	ILphenA	338	0.02
	LLCTphenB	335	0.02
	LLCTphenB/ILphenA	333	0.02
	MLCTphenA/LLCTphenB	330	0.04
	LLCTphenB/ILphenA	330	0.02
	LLCTphenB/ILphenB	325	0.02
	ILphenB/LLCTphenB	319	0.02
	ILphenB/LLCTphenB	315	0.03
	LLCTphenB/MLCTphenB	308	0.13
	LLCTphenA/LLCTphenB	305	0.02
	MLCTphenB	303	0.07
	MLCTphenB/LLCTphenB	297	0.44
	LLCTphenB	295	0.03
	MLCTphenB	295	0.22
	MLCTphenB	293	0.04
	ILphenB	285	0.14
	MLCTphenA	275	0.02
	ILphenB/LLCTphenA	273	0.04
	ILphenB/ILphenA	272	0.11
C6			
	MLCTphenB/MLCTphenA	492	0.03
	MLCTphenA	489	0.02
	MLCTphenA/MLCTphenB	466	0.02
	MLCTphenB/LLCTphenB	357	0.02
	MLCTphenA/ILphenA	355	0.08
	MLCTphenA/ILphenA	351	0.02
	MLCTphenA/ILphenA	332	0.07
	MLCTphenA/ILphenA	272	0.11
	MLCTphenA	272	0.03
	LLCTphenB/ILphenB	271	0.07
	ILphenB/LLCTphenB/MLCTphenB	271	0.26
	MLCTphenB	268	0.03
	MLCTphenA/ILphenB/ILphenA	267	0.04
	MLCTphenA/ILphenA	266	0.07
	LLCTphenB/ILphenA	265	0.07
	LLphenB/MLCTphenA/ILphenA	264	0.10
	MLCTphenB/LLCTphenB	262	0.03
	MLCTphenA/ILphenA	259	0.10
	MLCTphenA/ILphenA	256	0.10
	MLCTphenA/ILphenA	255	0.05

dx.doi.org/10.1021/ic2006343 |*Inorg. Chem.* 2011, 50, 11309–11322

Table 3. Continued

complex	state	ΔE (nm)	f
	MLCTphenA	254	0.03
	MLCTphenB/LLCTphenB	253	0.06
	LLCTphenB	253	0.02
	MLCTphenB/LLCTphenB	251	0.05
	MLCTphenB/LLCTphenB	247	0.03

[a] $Phen^A$ and $Phen^B$ refer respectively to mesityl and non-mesityl derivatized ligands.

The TD-DFT/B3LYP absorption spectra of **C3** and **C6** are presented in Figure 4. These two complexes contain a phenanthroline substituted in 2,9 positions by butyl groups (abbreviated $phen^B$) and another phenanthroline substituted in 2,9 positions by mesityl groups (abbreviated $phen^A$). The comparison with the above experimental spectra is not straightforward since the computations are performed in a vacuum for the isolated molecules. The TD-DFT solvent corrected absorption spectra will be presented elsewhere in an article devoted to the theoretical study where the methodological points will be discussed. The transition energies to the low-lying singlet excited states together with the associated oscillator strengths are reported in Table 3 for complexes **C3** and **C6**.

The two complexes are characterized by an intense absorption in the UV centered at 297 nm for complex **C3** and at 271 nm for complex **C6**. As mentioned above, this band corresponds to a mixed MLCT/LLCT state for complex **C3**, while it is a mixture of LLCT, IL, and MLCT transitions for complex **C6**. The shoulder around 500 nm corresponds to MLCT states localized on the $phen^A$ and $phen^B$ ligands in both complexes. The theoretical spectra are characterized by a peak around 350 nm, corresponding to the mixture of an IL state localized on the $phen^B$ ligand and an LLCT state for complex **C3**. In complex **C6**, this band is less intense, in agreement with experimental spectra, and corresponds to a mixed MLCT/IL state localized on $phen^A$. From the TD-DFT results, we may observe a very high density of states in this class of molecules, the nature and position of which are very sensitive to the substituents.

The main excitations of some characteristic excited states and related orbitals are shown in Table S2 and Figure S5 (Supporting Information), respectively.

Electrochemistry. All six complexes were studied by cyclic and square wave voltammetry in dry, argon purged dichloromethane. In all cases, a well-defined reversible oxidation wave was monitored and naturally assigned to the removal of one electron from the d orbitals of the copper(I) ion. The half-wave potentials were highly dependent on the extent of the steric hindrance at the $[Cu^I(phen^A)(phen^B)]^+$ core.[42] Indeed, the latter undergoes a shift from a tetrahedral to a square planar geometry when the oxidation number of the metal ion formally changes from +I to +II, respectively. Since mesityl, *n*-butyl, or methyl groups at the 2 and 9 positions of the phenanthroline moiety prevent such a deformation of the coordination cage, the oxidized form $[Cu^{II}(phen^A)(phen^B)]^{2+}$ (where $phen^B$ = Me-phen, nBu-phen or $\mathbf{L_2}$) is destabilized, and the potentials are overall anodically shifted. To summarize, the larger the steric hindrance, the higher the potential of the metal centered oxidation. This is indeed exemplified in our case since $E_{1/2}$ grows from 0.5 V for $[Cu^I(phen)_2]^+$ to 0.7 V for **C5** and finally reaches values between 0.85 and 1.05 V vs SCE for complexes **C1**, **C2**, **C3**, and **C4** where all ligands bear bulky substituents at positions 2 and 9 of the phenanthroline cores. The fact that methyl groups are less sterically demanding than *n*-butyl chains likely accounts for the 100 mV shift toward more positive potentials from **C1** to **C2**. Moreover, complexes **C3** and **C4** built with ligand $\mathbf{L_2}$ show a further increase in $E_{1/2}$; steric effects cannot be put forward here since the coordination spheres of **C2**, **C3**, and **C4** are virtually the same. Nevertheless, dppz is a well-known π-acceptor and exerts a strong electron withdrawing power, which could be held responsible for the anodic shift of the potentials for **C3** and **C4**.

The cathodic behavior of our complexes has been investigated within the limits imposed by the solvent used (dichloromethane) under our conditions. For complexes **C1**, **C2**, and **C5**, no reduction wave was observed, meaning that phenanthroline based reductions (or Cu(0) formation) occur at potentials below −1.6 V/SCE, a fact that is corroborated by the literature for similar complexes.[43,48] Conversely, the cathodic behavior of $\mathbf{L_2}$-built complexes **C3** and **C4** revealed, for both, a well-defined one-electron, reversible reduction wave at $E_{1/2}$ = −1.09 and −1.03 V vs SCE respectively. The shape of the wave, the value of the half wave potentials, and the apparent insensitivity of the latter to the complementary ligand ($\mathbf{L_1}$ or Mes-phen) are very reminiscent of those of other metal based dppz complexes, in particular the archetypal $[Ru^{II}(bpy)_2(dppz)]^{2+}$. We therefore assigned these reduction waves to the addition of an extra electron on the phenazine moiety. To further probe this assumption, we performed cathodic spectroelectrochemistry on complex **C3**. Upon electrolysis, several spectral changes are monitored (Figure 5); in particular, a broad shoulder around 560 nm, extending to 620 nm, is rising while the $\mathbf{L_2}$ centered $\pi-\pi^*$ transition at 275 nm collapses. These features are characteristic of (metal-bound) $dppz^{\bullet-}$ radical anion formation,[46] corroborating the initial assumption. Interestingly, the MLCT shows very little change, the intensity of which being only slightly enhanced, probably because of a spectral overlap with the 560 nm transition. This weak electronic coupling between the phenazine moiety and the "$Cu^I(phen)_2$" core is once again reminiscent of similar ruthenium complexes, and it seems therefore justified to consider complexes **C3** and, by extension, **C4** as bichromophoric systems. Additionally, several isosbestic points evidence the formation of only one species during the electrolysis, accounting for the stability of the reduced complex.

Photoluminescence Study. As mentioned in the Introduction, the main challenge to obtaining luminescent copper complexes is to avoid or minimize the flattening distortion of the complex from the Cu^I preferred tetrahedral geometry to the formal Cu^{II} square planar arrangement in the MLCT excited state.[3,4] In the flattened relaxed excited state, the complex has a smaller gap with the ground state, and the nonradiative decay is faster. Moreover, a very efficient quenching of the excited state by the solvent and exciplex formation can happen. Altogether, these two effects shorten the lifetime and luminescence quantum yield of the MLCT excited state. For example, while $[Cu^I(phen)_2]^+$ shows no luminescence at room temperature, the complex $[Cu^I(Me\text{-}phen)_2]^+$ containing methyl substituents in positions 2 and 9 of the phenanthroline emits at 730 nm and exhibits a luminescence quantum yield of about 4×10^{-4} with a time decay of about 90 ns in dichloromethane at room temperature.[10] The best example of sterically blocked distortion is given by the heteroleptic complex Cu^I(*tert*-butyl-phen)(Me-phen)$]^+$, in which the *tert*-butyl and methyl groups prevent the flattening and give a significant luminescence quantum yield of

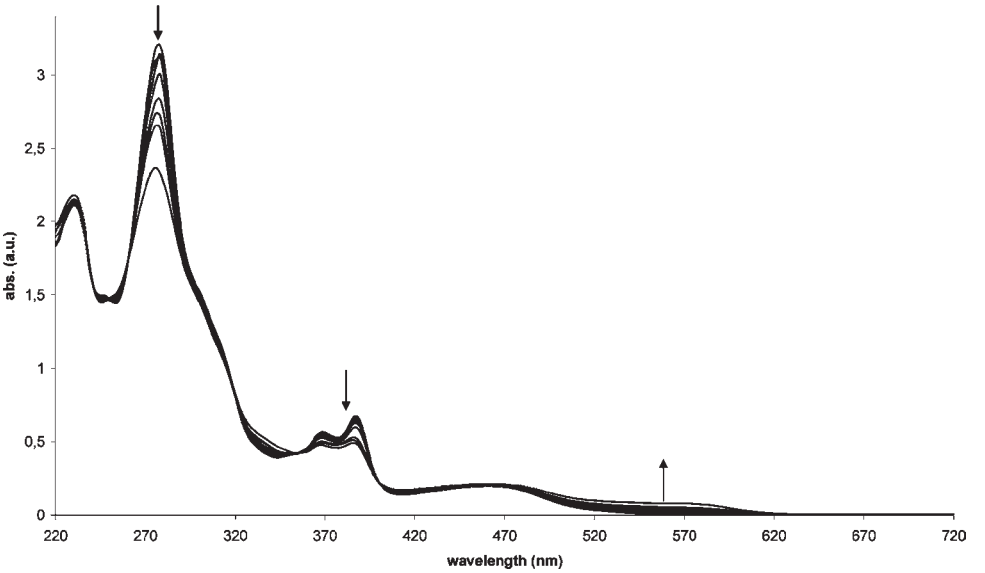

Figure 5. Evolution of the electronic absorption spectra of complex **C3** upon cathodic electrolysis (in dichloromethane, with 0.1 M tetra-*n*-butylammonium hexafluorophosphate as a supporting electrolyte and a platinum grid as the working electrode).

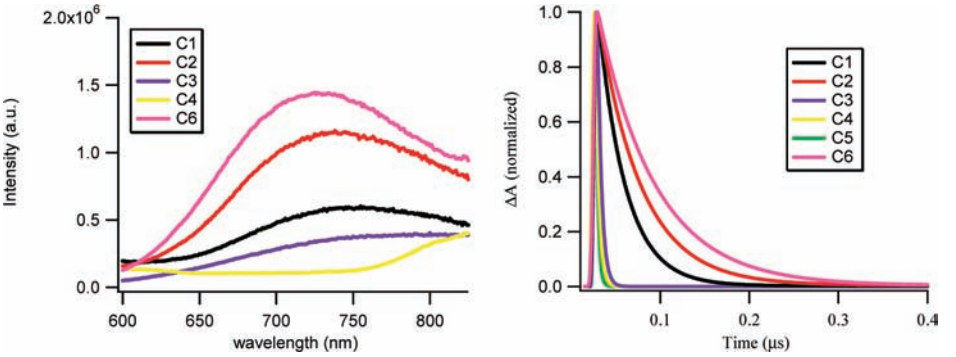

Figure 6. Emission spectra and excited-state time decay recorded in degassed dichloromethane for complexes **C1**−**C6** (excitation at 460 nm).

Table 4. Luminescence and Time Resolved Data for Complexes C1−C6[a]

	emission and excited state lifetime λ_{MLCT}/nm (τ/ns ±4 ns)		
complex	CH_2Cl_2	CH_3CN	absorption maximum of MLCT excited state in CH_2Cl_2/nm
C1	754 (31)	753 (21)	540
C2	740 (52)	743 (30)	550
C3	~ 800 (5)	nd (≤4)	630
C4	> 800 (≤4)	nd (≤4)	620
C5	nd (≤4)	nd (≤4)	550
C6	730 (64)	738 (25)	570

[a] All measurements were performed under degassed conditions. nd = not detected, very weak signal, and hardly distinguishable from the instrumental noise.

1% and a lifetime of 730 ns in dichloromethane.[17] The luminescence spectra and the lifetime of MLCT excited states for **C1**−**C6** are given in Figure 6, and the data are compiled in Table 4. These measurements were recorded in dichloromethane and acetonitrile, because these solvents have very different dielectric constants and coordination abilities. All measurements have been performed under the same conditions (absorbance at the excitation wavelength and instrumental parameters) to enable a straightforward and qualitative comparison of luminescence quantum yields.

A general trend is a slight bathochromic shift of the maximum emission wavelength and a shortening of the emission lifetime as we shift from dichloromethane to acetonitrile (Table 4). This is the consequence of the higher dielectric constant of acetonitrile, which stabilizes the charge transfer state, and its stronger coordinating ability, which increases exciplex quenching by pentacoordination of Cu(II). Heteroleptic complex **C6** was prepared to assess the influence of the fused heterocycle moiety capping the back of the phenanthroline. As the substituent size increases, within the series **C5**, **C1**, and **C2**, the emission lifetime of the MLCT naturally increases too, owing to restricted flattening of the excited state. The comparison of complex **C2** with reference complex **C6** indicates that the fused imidazole ring has little impact on the emission characteristic of the complex. On the other hand, the ligand $\mathbf{L_2}$ bearing the phenazine spacer has a

dx.doi.org/10.1021/ic2006343 |*Inorg. Chem.* 2011, 50, 11309–11322

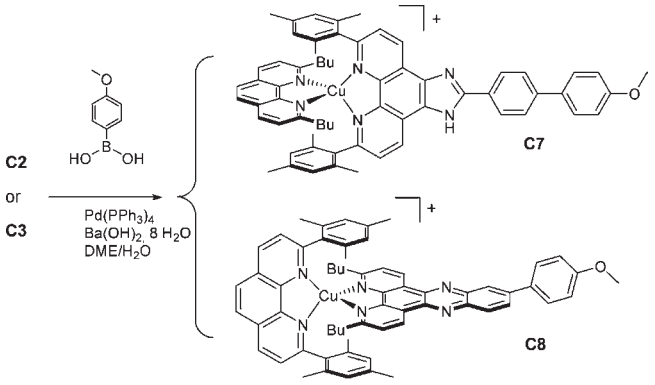

Figure 7. Suzuki cross-coupling reaction performed on complexes **C2** and **C3**, yielding **C7** and **C8**, respectively.

profound impact on the emission properties of the resulting copper(I) complexes **C3** and **C4**, the latter being barely emissive (Table 4).

Nanosecond transient absorption spectroscopy was used to follow the relaxation of the triplet MLCT excited-state (Figure S6, Supporting Information) for each complex. The transient trace of the MLCT excited state in these complexes is red-shifted relative to that of the other complexes (Figure S6), showing some resemblance with the spectrum of the radical anion of the complex **C3** recorded by spectro-electrochemistry (Figure 5). The photophysical properties of $[Ru^{II}(bpy)_2dppz]^{2+}$ were investigated in great detail,[18,49] and it is well-accepted that the dppz ligand can be considered a weakly coupled dyad in which the pyrido and phenazine units behave quite independently. The emission lifetime of the complex $[Ru^{II}(bpy)_2dppz]^{2+}$ is decreased relative to that of $[Ru^{II}(bpy)_3]^{2+}$ owing to the quenching of the MLCT excited state by electron transfer to the phenazine π-accepting unit. In addition, hydrogen bonding between the dppz and a protic solvent is another cause of the excited-state quenching of the MLCT excited state. With reference to these studies on $[Ru^{II}(bpy)_2dppz]^{2+}$, and with the support of the transient emission and absorption studies, the quenching of the MLCT luminescence in **C3** and **C4** is likely to due to a photoinduced electron transfer from Cu(I) to phenazine. The charge separated state is however very short-lived, since recombination occurs on the nanosecond time scale. This is nevertheless an encouraging feature, legitimating the possibility of copper(I)−phenanthroline based photochemistry.

Chemistry on the Complex. Thanks to the HETPHEN concept, many intricate supramolecular structures were obtained with minimal synthetic effort.[9,13,15,39,50,51] It would be therefore particularly appealing to know whether chemical alteration is possible on such assemblies, without degrading the integrity of the latter: copper(I) phenanthroline complexes are indeed well-known to be kinetically labile, and their stability is at stake when they are in the presence of any other potential ligand, like a mere Lewis base. Encouragingly, a copper catalyzed Glaser homocoupling[39] and a Sonogashira cross-coupling[50] were reported too, although in the latter case a "kinetically locked" copper complex was used.[52] "Click chemistry" has been performed too on catenanes,[53] assembled *via* coordination of copper(I) by two phenanthroline cavities. Complexes **C1**−**C4** are nevertheless more sterically challenged and therefore potentially less stable than catenanes, and it is also necessary to test the stability of heteroleptic copper complexes in the presence of a different catalyst than Cu^{n+} ($n = 0$, 1, or 2). In order to assess this last point, we involved two of our bromo terminated copper complexes in a palladium catalyzed cross-coupling Suzuki reaction. The latter was chosen with regard to its high impact in modern organic chemistry and great versatility, giving access to a plethora of structures and new functionalities. As a proof of concept, *para*-methoxy phenyl boronic acid was thus engaged in a Suzuki coupling reaction with complexes **C2** and **C3** (Figure 7). A classical procedure (catalytic $Pd(PPh_3)_4$ and $Ba(OH)_2 \cdot 8H_2O$ in a refluxing 4:1 mixture of DME/H_2O overnight) appeared to be successful, affording complexes **C7** and **C8** with yields of 34% and 84%, respectively. The higher yield for **C8** than **C7** can be rationalized by the greater activation of the C−Br bond, given the electron withdrawing character of phenazine. It is important to notice that, however, a small amount of homoleptic complex was formed through the course of the reaction, which could not be removed by chromatography owing to very similar mobilities on the stationary phase, and prevented us from getting satisfactory microanalysis.

Stability Assessment. The small, yet significant amount of homoleptic complex formed during the Suzuki cross coupling reactions unveiled a possible stability issue of our heteroleptic systems. A series of tests was therefore undertaken, with the model complex **C6**. When the latter is dissolved and heated in dichloromethane (apolar, noncoordinating) or acetonitrile (polar, coordinating), no $[Cu^{I}(n\text{Bu-phen})_2]^{+}$ was detected by ^1H NMR, even after several hours of heat (and light) stress, which tends to confirm the stability of **C6**, and by extrapolation of any heteroleptic complex with a related structure. However, in the presence of excess *n*Bu-phen, the heteroleptic complex spontaneously dissociates to yield the homoleptic complex $[Cu^{I}(n\text{-Bu-phen})_2]^{+}$. A quantitative analysis of the ^1H NMR data revealed that the homoleptic species is approximately 7 times more stable than **C6** (Figures S7−S9, Supportng Information). The HETPHEN concept states that heteroleptic copper complexes are stable, thanks to the bulkiness of mesityl groups, but in the presence of an exogenous ligand, capable of yielding homoleptic complexes (typically here, *n*-Bu-phen), a fast ligand exchange occurs, owing to the well-known lability of such species. Eventually, the more thermodynamically stable complex is formed. In our case, the *n*-butyl groups are believed to enhance the σ-donating ability of the phenanthroline chelate and therefore stabilize $[Cu^{I}(n\text{Bu-phen})_2]^{+}$ vs **C6**. The higher steric bulk in **C6** might account for a lesser stability too, compared to the less sterically stringed homoleptic complex. Comparing the optimized structure of $[Cu^{I}(n\text{Bu-phen})_2]^{+}$ and **C6** using the DFT/PBE-D method, $[Cu^{I}(n\text{Bu-phen})_2]^{+}$ has shorter Cu−N bonds (Cu−N_1, 2.021 Å; Cu−N_2, 2.021 Å; Cu−N_3, 2.023 Å; Cu−N_4, 2.023 Å) than those of **C6** (Table 1) on average. $[Cu^{I}(n\text{-Bu-phen})_2]^{+}$ has an almost symmetric structure (N_1−Cu−N_2, 82.87°; N_3−Cu−N_4, 82.66°; N_1−Cu−N_3, 124.23°; N_1−Cu−N_4, 124.34°; N_2−Cu−N_3, 124.34°; N_2−Cu−N_4, 124.23°) and from the viewpoint of coordination, this complex is more stable than the π-stacking **C6** complex. In addition to this, when *n*-Bu-phen, Mes-phen, and $[Cu(CH_3CN)_4]PF_6$ are all mixed together in dichloromethane, a mixture of homo- and heteroleptic complexes is obtained. **C6** happens to be the major species formed in this rather kinetically controlled experiment, but should polar and coordinating acetonitrile or DME be used as solvents instead of dichloromethane, that the trend would be inverted (Figures S7−S9). It is henceforth of paramount importance to respect the order of introduction of the different reactants, to avoid the formation of the undesired homoleptic complex. Under the Suzuki reaction conditions, DME, H_2O, and

PPh_3 are all potentially coordinating and could be involved in ligand exchange reactions, leading eventually to the formation of the homoleptic species. Nevertheless, only 5% of the latter was formed under rather harsh, nonoptimized conditions (120 °C), asserting that a careful choice of reactants and reaction conditions should allow for performing chemistry on the complex.

CONCLUSIONS

This work stands within the frame of unveiling the synthesis of copper(I) phenanthroline complexes and their physicochemical properties. To achieve this goal, two bulky original ligands, $\mathbf{L_1}$ and $\mathbf{L_2}$, were synthesized. $\mathbf{L_1}$ results from the fusion of a benzimidazole skeleton with the bulky 2,9-dimesityl-1,10-phenanthroline. The structure of $\mathbf{L_2}$ stems from the well-known dppz, bearing two *n*-butyl chains in α positions of the chelating nitrogen atoms. Both ligands provide a strong steric bulk at the copper center, leading to the obtaining of heteroleptic complexes by combination of $\mathbf{L_1}$ and $\mathbf{L_2}$ with adequate phenanthroline derivatives, thanks to the HETPHEN concept developed by Schmittel and co-workers. In spite of the lability of phenanthroline ligands coordinated to copper(I), a palladium catalyzed cross-coupling reaction has been successfully performed, directly on the complex, with only marginal damage on the starting molecules. With complex **C3**, the copper(I) cation is in a distorted tetrahedral arrangement, due to π-stacking between mesityl groups and the neighboring dppz ligand. Additionally, most welcome stability is thus provided to the complex. From one ligand to the other, the arrangement is basically linear, which is a particularly important feature of copper(I)−phenanthroline complexes, paving the way to optimized acceptor−donor photosensitive devices. The new complexes were characterized by electrochemistry, UV−vis absorption spectra, steady state and time-resolved luminescence spectroscopy, and pump−probe transient spectroscopy and fully interpreted with the aid of DFT quantum chemical calculations. The electron attracting character of the phenazine unit in ligand $\mathbf{L_2}$ leads to fast nonradiative quenching of the MLCT excited-state of the corresponding copper(I) complexes, whereas for the mesityl bulky subtituents in ligand $\mathbf{L_1}$, a luminescence quantum yield of about 3×10^{-4} is obtained, with a decay time of about 50 ns for **C2** measured. Therefore, the latter complex has a potential use as a sensitizer for the design of molecular arrays for photoinduced charge separation. Work is in progress in our groups toward this goal.

ASSOCIATED CONTENT

Supporting Information. ^{1}H NMR spectra of the ligand $\mathbf{L_1}$ and of complexes **C1**−**C6**, X-ray structure of complex **C3**, the representation and the nature of the orbitals involved in the optical transitions for complexes **C3** and **C6**, the transient absorption spectra of complexes **C1**−**C6**, the stability assessment for complex **C6**, and the Cartesian coordinates of the optimized structures of the complexes **C1**−**C6**. This material is available free of charge via the Internet at http://pubs.acs.org.

AUTHOR INFORMATION

Corresponding Author

*Tel.: +33 368 851314 (C.D.), +33 251125429 (F.O.). Fax: +33 368851589 (C.D.), +33 251125402 (F.O.). E-mail: michel.evain@univ-nantes.fr, c.daniel@chimie.u-strasbg.fr, Fabrice.Odobel@univ-nantes.fr.

ACKNOWLEDGMENT

The "Agence Nationale de la Recherche" (ANR) is gratefully acknowledged for the financial support of this research through the "Programme Blanc" entitled "HeteroCop" referenced ANR-09-BLAN-0183-01. These studies were also supported by the European program COST D35. F.O. warmly thanks Benoit Colasson (Université Paris Descartes) for fruitful and inspiring discussions about the present work. The calculations were carried out in part at the IDRIS and CINES computer centers through a grant of computer time from the Conseil Scientifique.

REFERENCES

(1) Dietrich-Buchecker, C. O.; Marnot, P. A.; Sauvage, J. P.; Kirchoff, J. R.; McMillin, D. R. *Chem. Commun.* **1983**, 513. Gushurst, A. K. I.; McMillin, D. R.; Dietrich-Buchecker, C. O.; Sauvage, J. P. *Inorg. Chem.* **1989**, *28*, 4070. Blasse, G.; Breddels, P. A.; McMillin, D. R. *Chem. Phys. Lett.* **1984**, *109*, 24. Blaskie, M. W.; McMillin, D. R. *Inorg. Chem.* **1980**, *19*, 3519.McMillin, D. R.; Gamache, R. E., Jr.; Kirchhoff, J. R.; Del, P. A. A. In *Photochemical and Photophysical Studies of Copper(I) Complexes*; Adenine Press: Schenectady, NY, 1983; p 223. Buckner, M. T.; McMillin, D. R. *Chem. Commun.* **1978**, 759. McMillin, D. R.; Kirchhoff, J. R.; Goodwin, K. V. *Coord. Chem. Rev.* **1985**, *64*, 83. Everly, R. M.; Ziessel, R.; Suffert, J.; McMillin, D. R. *Inorg. Chem.* **1991**, *30*, 559.

(2) Ichinaga, A. K.; Kirchhoff, J. R.; McMillin, D. R.; Dietrich-Buchecker, C. O.; Marnot, P. A.; Sauvage, J. P. *Inorg. Chem.* **1987**, *26*, 4290.

(3) Armaroli, N. *Chem. Soc. Rev.* **2001**, *30*, 113.

(4) Armaroli, N.; Accorsi, G.; Cardinali, F.; Listorti, A. *Top. Curr. Chem.* **2007**, *280*, 69.

(5) Lavie-Cambot, A.; Cantuel, M.; Leydet, Y.; Jonusauskas, G.; Bassani, D. M.; McClenaghan, N. D. *Coord. Chem. Rev.* **2008**, *252*, 2572. Horváth, O. *Coord. Chem. Rev.* **1994**, *135*−*136*, 303.

(6) McGarvey, J. J.; Bell, S. E. J.; Bechara, J. N. *Inorg. Chem.* **1986**, *25*, 4325. McGarvey, J. J.; Bell, S. E. J.; Gordon, K. C. *Inorg. Chem.* **1988**, *27*, 4003.

(7) Campagna, S.; Puntoriero, F.; Nastasi, F.; Bergamini, G.; Balzani, V. *Top. Curr. Chem.* **2007**, *280*, 117. Sauvage, J. P.; Collin, J. P.; Chambron, J. C.; Guillerez, S.; Coudret, C.; Balzani, V.; Barigelletti, F.; De Cola, L.; Flamigni, L. *Chem. Rev.* **1994**, *94*, 993. Medlycott, E. A.; Hanan, G. S. *Chem. Soc. Rev.* **2005**, *34*, 133. Abrahamsson, M.; Jager, M.; Kumar Rohan, J.; Osterman, T.; Persson, P.; Becker, H.-C.; Johansson, O.; Hammarström, L. *J. Am. Chem. Soc.* **2008**, *130*, 15533.

(8) Polo, A. S.; Itokazu, M. K.; Murakami Iha, N. Y. *Coord. Chem. Rev.* **2004**, *248*, 1343.

(9) Schmittel, M.; Ganz, A. *Synlett* **1997**, 710.

(10) Schmittel, M.; Ganz, A. *Chem. Commun.* **1997**, 1815. Schmittel, M.; Ganz, A.; Fenske, D.; Herderich, M. *Dalton Trans.* **2000**, 353.

(11) Schmittel, M.; Michel, C.; Liu, S.-X.; Schildbach, D.; Fenske, D. *Eur. J. Inorg. Chem.* **2001**, 1155.

(12) De, S.; Mahata, K.; Schmittel, M. *Chem. Soc. Rev.* **2010**, *39*, 1555.

(13) Kalsani, V.; Bodenstedt, H.; Fenske, D.; Schmittel, M. *Eur. J. Inorg. Chem.* **2005**, 1841.

(14) Schmittel, M.; Kishore, R. S. K.; Bats, J. W. *Org. Biomol. Chem.* **2007**, *5*, 78.

(15) Kalsani, V.; Ammon, H.; Jäckel, F.; Rabe, J. P.; Schmittel, M. *Chem.— Eur. J.* **2004**, *10*, 5481.

(16) Schmittel, M.; Ganz, A.; Fenske, D. *Org. Lett.* **2002**, *4*, 2289.

(17) Miller, M. T.; Gantzel, P. K.; Karpishin, T. B. *J. Am. Chem. Soc.* **1999**, *121*, 4292.

(18) Chambron, J. C.; Sauvage, J. P.; Amouyal, E.; Koffi, P. *Nouv. J. Chim.* **1985**, *9*, 527.

(19) Konduri, R.; Ye, H.; MacDonnell, F. M.; Serroni, S.; Campagna, S.; Rajeshwar, K. *Angew. Chem., Int. Ed.* **2002**, *41*, 3185. Chiorboli, C.; Bignozzi, C. A.; Scandola, F.; Ishow, E.; Gourdon, A.; Launay, J.-P. *Inorg. Chem.* **1999**, *38*, 2402. Chiorboli, C.; Fracasso, S.; Scandola, F.;

Campagna, S.; Serroni, S.; Konduri, R.; MacDonnell, F. M. *Chem. Commun.* **2003**, 1658. Goze, C.; Leiggener, C.; Liu, S.-X.; Sanguinet, L.; Levillain, E.; Hauser, A.; Decurtins, S. *ChemPhysChem* **2007**, *8*, 1504. Rau, S.; Schaefer, B.; Gleich, D.; Anders, E.; Rudolph, M.; Friedrich, M.; Goerls, H.; Henry, W.; Vos, J. G. *Angew. Chem., Int. Ed.* **2006**, *45*, 6215.

(20) Lundin, N. J.; Walsh, P. J.; Howell, S. L.; McGarvey, J. J.; Blackman, A. G.; Gordon, K. C. *Inorg. Chem.* **2005**, *44*, 3551.

(21) Lim, M. H.; Song, H.; Olmon, E. D.; Dervan, E. E.; Barton, J. K. *Inorg. Chem.* **2009**, *48*, 5392. Rueba, E.; Hart, J. R.; Barton, J. K. *Inorg. Chem.* **2004**, *43*, 4570. Delaney, S.; Pascaly, M.; Bhattacharya, P. K.; Han, K.; Barton, J. K. *Inorg. Chem.* **2002**, *41*, 1966. Jenkins, Y.; Friedman, A. E.; Turro, N. J.; Barton, J. K. *Biochemistry* **1992**, *31*, 10809. Sentagne, C.; Chambron, J.-C.; Sauvage, J.-P.; Paillous, N. *J. Photochem. Photobiol., B* **1994**, *26*, 165.

(22) Frey, J.; Kraus, T.; Heitz, V.; Sauvage, J.-P. *Chem.—Eur. J.* **2007**, *13*, 7584.

(23) Grimme, S. *J. Comput. Chem.* **2006**, *27*, 1787.

(24) van Lenthe, E.; J., B. E. *J. Comput. Chem.* **2003**, *24*, 1142.

(25) *Amsterdam Density Functional program*; Theoretical Chemistry, Vrije Universiteit: Amsterdam. http://www.scm.com (accessed October 2011). te Velde, G.; Bickelhaupt, F. M.; Baerends, E. J.; Guerra, C. F.; van Gisbergen, S. J. A.; Snijders, J. G.; Ziegler, T. *J. Comput. Chem.* **2001**, *22*, 931.

(26) Petersilka, M.; Gossmann, U. J.; Gross, E. K. U. *Phys. Rev. Lett.* **1996**, *76*, 1212.

(27) Becke, A. D. *J. Chem. Phys.* **1993**, *98*, 5648. Gross, E. K. U.; Kohn, W. *Phys. Rev. Lett.* **1985**, *55*, 2850. Gorling, A.; Heinze, H. H.; Ruzankin, S. P.; Staufer, M.; Rosch, N. *J. Chem. Phys.* **1999**, *110*, 2785.

(28) Dunning, T. H., Jr. *J. Chem. Phys.* **1989**, *90*, 1007.

(29) Bera, N. C.; Bhattacharyya, I.; Das, A. K. *Spectrochim. Acta, Part A* **2007**, *67A*, 894.

(30) Frisch, M. J. T. G. W.; Schlegel, H. B.; Scuseria, G. E.; Robb, M. A.; Cheeseman, J. R.; Montgomery, J. A., Jr.; Vreven, T.; Kudin, K. N.; Burant, J. C.; Millam, J. M.; Iyengar, S. S.; Tomasi, J.; Barone, V.; Mennucci, B.; Cossi, M.; Scalmani, G.; Rega, N.; Petersson, G. A.; Nakatsuji, H.; Hada, M.; Ehara, M.; Toyota, K.; Fukuda, R.; Hasegawa, J.; Ishida, M.; Nakajima, T.; Honda, Y.; Kitao, O.; Nakai, H.; Klene, M.; Li, X.; Knox, J. E.; Hratchian, H. P.; Cross, J. B.; Bakken, V.; Adamo, C.; Jaramillo, J.; Gomperts, R.; Stratmann, R. E.; Yazyev, O.; Austin, A. J.; Cammi, R. P. C.; Ochterski, J. W.; Ayala, P. Y.; Morokuma, K.; Voth, G. A.; Salvador, P.; Dannenberg, J. J.; Zakrzewski, V. G.; Dapprich, S.; Daniels, A. D.; Strain, M. C.; Farkas, O.; Malick, D. K.; Rabuck, A. D.; Raghavachari, K.; Foresman, J. B.; Ortiz, J. V.; Cui, Q.; Baboul, A. G.; Clifford, S.; Cioslowski, J.; Stefanov, B. B.; Liu, G.; Liashenko, A.; Piskorz, P.; Komaromi, I.; Martin, R. L.; Fox, D. J.; Keith, T.; Al-Laham, M. A.; Peng, C. Y.; Nanayakkara, A.; Challacombe, M.; Gill, P. M. W.; Johnson, B.; Chen, W.; Wong, M. W.; Gonzalez, C.; Pople, J. A. Gaussian, Inc.: Wallingford, CT, 2005.

(31) Oszlanyi, G.; Sueto, A. *Acta Crystallogr., Sect. A* **2004**, *A60*, 134.

(32) Palatinus, L.; Chapuis, G. *J. Appl. Crystallogr.* **2007**, *40*, 786.

(33) Petricek, V.; Dusek, M.; Palatinus, L. *Jana2006*: The crystallographic computing system, Institute of Physics: Praha, Czech Republic, 2006.

(34) Ott, S.; Faust, R. *Synthesis* **2005**, 3135.

(35) Pallenberg, A. J.; Koenig, K. S.; Barnhart, D. M. *Inorg. Chem.* **1995**, *34*, 2833.

(36) Yamada, M.; Nakamura, Y.; Kuroda, S.; Shimao, I. *Bull. Chem. Soc. Jpn.* **1990**, *63*, 2710. Yamada, M.; Tanaka, Y.; Yoshimoto, Y.; Kuroda, S.; Shimao, I. *Bull. Chem. Soc. Jpn.* **1992**, *65*, 1006.

(37) Steck, E. A.; Day, A. R. *J. Am. Chem. Soc.* **1946**, *68*, 771.

(38) Miller, M. T.; Gantzel, P. K.; Karpishin, T. B. *Inorg. Chem.* **1998**, *37*, 2285.

(39) Schmittel, M.; Kalsani, V.; Bats, J. W. *Inorg. Chem.* **2005**, *44*, 4115.

(40) Kubas, G. J. *Inorg. Synth.* **1979**, *19*, 90.

(41) Cunningham, C. T.; Moore, J. J.; Cunningham, K. L. H.; Fanwick, P. E.; McMillin, D. R. *Inorg. Chem.* **2000**, *39*, 3638.

(42) Miller, M. T.; Gantzel, P. K.; Karpishin, T. B. *Inorg. Chem.* **1999**, *38*, 3414.

(43) Eggleston, M. K.; McMillin, D. R.; Koenig, K. S.; Pallenberg, A. J. *Inorg. Chem.* **1997**, *36*, 172.

(44) Miller, M. T.; Karpishin, T. B. *Inorg. Chem.* **1999**, *38*, 5246.

(45) Ackermann, M. N.; Interrante, L. V. *Inorg. Chem.* **1984**, *23*, 3904.

(46) Fees, J.; Kaim, W.; Moscherosch, M.; Matheis, W.; Klima, J.; Krejcik, M.; Zalis, S. *Inorg. Chem.* **1993**, *32*, 166.

(47) Phifer, C. C.; McMillin, D. R. *Inorg. Chem.* **1986**, *25*, 1329.

(48) Masood, M. A.; Zacharias, P. S. *J. Chem. Soc., Dalton Trans.* **1991**, 111.

(49) Olofsson, J.; Önfelt, B.; Lincoln, P. *J. Phys. Chem. A* **2004**, *108*, 4391. Brennaman, M. K.; Alstrum-Acevedo, J. H.; Fleming, C. N.; Jang, P.; Meyer, T. J.; Papanikolas, J. M. *J. Am. Chem. Soc.* **2002**, *124*, 15094. Önfelt, B.; Lincoln, P.; Norden, B.; Baskin, J. S.; Zewail, A. H. *Proc. Natl. Acad. Sci. U S A* **2000**, *97*, 5708.

(50) Schmittel, M.; Mahata, K. *Chem. Commun.* **2008**, 2550.

(51) Mahata, K.; Schmittel, M. *J. Am. Chem. Soc.* **2009**, *131*, 16544. Schmittel, M.; He, B.; Kalsani, V.; Bats, J. W. *Org. Biomol. Chem.* **2007**, *5*, 2395. Schmittel, M.; Mal, P. *Chem. Commun.* **2008**, 960.

(52) Kalsani, V.; Schmittel, M.; Listorti, A.; Accorsi, G.; Armaroli, N. *Inorg. Chem.* **2006**, *45*, 2061.

(53) Durot, S.; Mobian, P.; Collin, J.-P.; Sauvage, J.-P. *Tetrahedron* **2008**, *64*, 8496.